frontiers in Plant Science

ORIGINAL RESEARCH
published: 18 September 2019
doi: 10.3389/fpls.2019.01104

# Complex Horticultural Quality Traits in Broccoli Are Illuminated by Evaluation of the Immortal BolTBDH Mapping Population

*Zachary Stansell*[1,2]*, *Mark Farnham*[3] *and Thomas Björkman*[1,2]

[1] School of Integrative Plant Science, Cornell University, Ithaca, NY, United States, [2] Cornell Agritech, Cornell University, Geneva, NY, United States, [3] USDA-ARS Vegetable Laboratory, Department of Horticulture, Charleston, SC, United States

OPEN ACCESS

**Edited by:**
*Ryo Fujimoto,*
*Kobe University, Japan*

**Reviewed by:**
*Zhansheng Li,*
*Institute of Vegetables and Flowers (CAAS), China*
*Takahiro Kawanabe,*
*Tokai University, Japan*

***Correspondence:**
*Zachary Stansell*
*Zjs29@cornell.edu*

**Specialty section:**
*This article was submitted to Plant Breeding, a section of the journal Frontiers in Plant Science*

**Received:** *28 June 2019*
**Accepted:** *12 August 2019*
**Published:** *18 September 2019*

**Citation:**
*Stansell Z, Farnham M and Björkman T (2019) Complex Horticultural Quality Traits in Broccoli Are Illuminated by Evaluation of the Immortal BolTBDH Mapping Population. Front. Plant Sci. 10:1104. doi: 10.3389/fpls.2019.01104*

Improving horticultural quality in regionally adapted broccoli (*Brassica oleracea* var. *italica*) and other *B. oleracea* crops is challenging due to complex genetic control of traits affecting morphology, development, and yield. Mapping horticultural quality traits to genomic loci is an essential step in these improvement efforts. Understanding the mechanisms underlying horticultural quality enables multi-trait marker-assisted selection for improved, resilient, and regionally adapted *B. oleracea* germplasm. The publicly-available biparental double-haploid BolTBDH mapping population (Chinese kale × broccoli; $N$ = 175) was evaluated for 25 horticultural traits in six trait classes (architecture, biomass, phenology, leaf morphology, floral morphology, and head quality) by multiple quantitative trait loci mapping using 1,881 genotype-by-sequencing derived single nucleotide polymorphisms. The physical locations of 56 single and 41 epistatic quantitative trait locus (QTL) were identified. Four head quality QTL (OQ_C03@57.0, OQ_C04@33.3, OQ_CC08@25.5, and OQ_C09@49.7) explain a cumulative 81.9% of phenotypic variance in the broccoli heading phenotype, contain the *FLOWERING LOCUS C* (*FLC*) homologs Bo9g173400 and Bo9g173370, and exhibit epistatic effects. Three key genomic hotspots associated with pleiotropic control of the broccoli heading phenotype were identified. One phenology hotspot reduces days to flowering by 7.0 days and includes an additional *FLC* homolog Bo3g024250 that does not exhibit epistatic effects with the three horticultural quality hotspots. Strong candidates for other horticultural traits were identified: *BoLMI1* (Bo3g002560) associated with serrated leaf margins and leaf apex shape, *BoCCD4* (Bo3g158650) implicated in flower color, and *BoAP2* (Bo1g004960) implicated in the hooked sepal horticultural trait. The BolTBDH population provides a framework for *B. oleracea* improvement by targeting key genomic loci contributing to high horticultural quality broccoli and enabling *de novo* mapping of currently unexplored traits.

**Keywords: *Brassica olecarea* var. *italica*, broccoli, BolTBDH, genotype-by-sequencing, QTL mapping, complex horticultural traits, BoFLC, "TO1000"**

## INTRODUCTION

Improvement of broccoli and other *Brassica oleracea* vegetables (cauliflower, cabbage, kale, Gai lan, Brussels sprouts, kohlrabi, and collard) is constrained by complex interactions of many genes affecting plant architecture, developmental processes, and yield. *B. oleracea* vegetable crop groups have benefited from a number of advances in plant biotechnology, gradually increasing the overall understanding of these quality-based traits. Specifically, diversity and domestication processes (Cheng et al., 2016; Stansell et al., 2018; Yousef et al., 2018; Li et al., 2019) have been clarified, next-generation sequencing and high-quality reference genomes (Liu et al., 2014; Parkin et al., 2014; Golicz et al., 2016) have expedited discovery of molecular markers associated with key traits, and diverse mapping populations segregating for these traits have been characterized (Kianian and Quiros, 1992; Landry et al., 1992; Camargo and Osborn, 1996; Ramsay et al., 1996; Bohuon et al., 1998; Hu et al., 1998; Lan and Paterson, 2000; Sebastian et al., 2000; Lan and Paterson, 2001; Axelsson et al., 2001; Li et al., 2003; Gao et al., 2007; Brown et al., 2014; Lee et al., 2015a; Li et al., 2015). For example, projects integrating these tools such as the Eastern Broccoli Project (SCRI No. 2010-51181-21062) and the USDA Vegetable Brassica Research Project (CRIS No. 6080-21000-019-00D) have developed heat-tolerant broccoli germplasm adapted to novel environments, reducing costs and enabling more sustainable production models (Atallah et al., 2014; Farnham and Björkman, 2011).

A current limitation in *B. oleracea* vegetable crop improvement is a lack of publicly available mapping populations, constraining information integration across research programs. Attempts to unify existing maps have been limited due to variable germplasm, different marker types, and linkage group nomenclature (Hu et al., 1998). Furthermore, these populations are often difficult to maintain due to self-incompatibility (Farnham, 1998; Bohuon et al., 1998; Sebastian et al., 2000; Pink et al., 2008; Walley et al., 2012).

To address these issues, the double-haploid (DH) BolTBDH population was developed from a cross between morphologically distinct parents (*B. oleracea* var. *alboglabra* × *B. oleracea* var. *italica*) that segregates for horticultural quality traits specific to broccoli (Iniguez-Luy et al., 2009). BolTBDH offers several distinct advantages over other mapping populations: a large sample size (*N*~175), a high degree of self-compatibility, and a short generation time. The rapid-cycling parental taxa 'TO1000DH3' ($P_1$; var. alboglabra) is the reference organism for the *B. oleracea* v.2 genome (Parkin et al., 2014). 'Early Big' ($P_2$; var. *italica*) has been evaluated in previous studies (Li et al., 2003; Gao et al., 2005; Tortosa et al., 2018). Moreover, both $P_1$ and $P_2$ and included in the *B. oleracea* pangenome (Golicz et al., 2016). Furthermore, this population has already been used to investigate the genetic control of important traits: glucosinolate content (Sotelo et al., 2014), organ-specific phenylpropanoid metabolism (Francisco et al., 2016), antioxidant content (Sotelo Pérez et al., 2014), and black rot (*Xanthomonas campestris* pv. *campestris*) resistance (Iglesias-Bernabé et al., 2019). Under standard greenhouse conditions, BolTBDH lines will typically produce self-seed without the need for hand pollinations. The work presented here increases the value of this population by generating many high-quality genome-wide SNP markers and generating robust phenotypes for 25 horticultural quality traits.

The BolTBDH population provides an unique opportunity to evaluate the genetic basis of the heading broccoli phenotype due to the marked dissimilarity between the parental lines: $P_1$ is rapid-flowering (~ 65 days to flowering) and exhibits a leafy, non-head-forming inflorescence, whereas $P_2$ is relatively late-flowering (~ 85 days to flowering) and exhibits a heading broccoli phenotype characterized by extensive meristem proliferation during floral bud development and internode elongation (Björkman and Pearson, 1998). While considerable work has investigated head formation under optimal and heat-stressed conditions (Duclos and Björkman, 2008; Farnham and Björkman, 2011; Hasan et al., 2016; Lin et al., 2019), the exact genetic basis of this phenotype remains elusive (Axelsson et al., 2001; Li et al., 2003; Gao et al., 2007; Okazaki et al., 2007; Razi et al., 2008; Matschegewski et al., 2015; Irwin et al., 2016). There is a growing consensus of the central importance of the homologous flowering timing MADS-box transcription factor *FLOWERING LOCUS C* (*BoFLC*) in regulating the reproductive transition by inhibiting downstream *BoSOC1* and *BoFT* expression; in turn, delaying a suite of floral-identity genes including *BoLFY*, *BoAP1*, and *BoCAL* (Lin et al., 2018). The genetic basis of the heading broccoli phenotype could be explained by a number of models: simple control by one or several genes, a constrictive-conditional model where multiple genetic factors must be present, or a pleiotropic model, where several key developmental genes would underlie the broccoli heading phenotype and be further modified by additional downstream factors. Under a simple control model, the heading broccoli phenotype would exhibit qualitative control by a limited number of QTL. Under a purely constrictive-conditional model, the broccoli heading phenotype would occur only when a minimum set of independent factors were present. Under a purely pleiotropic model, a small number of developmental loci or genes are implicated in heading quality traits with epistatic interactions with additional loci.

When breeding multiple quality traits in horticultural crops, it is often challenging to determine the degree that individual traits contribute to the overall quality of these crops when predictor traits are correlated. Relative-importance analyses (RIA) allows quantification of the proportional contribution of a predictor variable to the overall quality-model $R^2$, considering both unique and joint contributions with other variables (Gromping, 2006) and may be used to establish breeding priorities within a horticultural context (Stansell et al., 2017). Within this study, RIA was used to evaluate the independent contribution of individual traits to overall horticultural quality.

Therefore, our main objectives were to: a) characterize the phenotypic variation of horticulturally important traits within the BolTBDH population; b) produce a reference set of robust and high-quality BolTBDH markers; c) identify optimal QTL models to best explain key horticultural quality traits important to broccoli germplasm; and d) identify which candidate *B. oleracea* developmental genes collocate with observed QTL.

# MATERIALS AND METHODS

## Germplasm

The BolTBDH population was generated *via* anther culture from the parental lines 'TO1000DH3' DH ($P_1$; *B. oleracea* var. *alboglabra*) × 'Early Big' DH ($P_1$; *B. oleracea* var. *italica*) (Iniguez-Luy et al., 2009). Seed was provided by the USDA Vegetable Laboratory in Charleston, SC. All initial lines ($N$ = 202; $P_1$ and $P_1$ inclusive) were increased in 2016 and closed-bud pollinations were made to verify selfing integrity. Except for $P_1$ in $Y_1$ due to inadequate seed quality, all lines were sown into 128 cell trays May 11 in $Y_1$ and May 9 in $Y_2$. Seedlings were grown in a greenhouse and transplanted into Lima silt loam fields in Geneva, NY on May 28–29 in $Y_1$ and June 8–11 in $Y_2$. All lines were divided into four randomized replications and transplanted onto raised beds with each plot containing 10–12 plants per genotype. Drip irrigation was applied as needed and any additional cultural practices were as previously described (Farnham and Björkman, 2011). Hourly weather data was collected locally at Cornell AgriTech (**Figure S1**).

## Traits Investigated

Plots were evaluated daily and deemed mature when 1/3 of the plants reached a heading or heading-equivalent stage. Traits within six classes considered important to broccoli or other *B. oleracea* crop groups were chosen: architecture, biomass, bud morphology, leaf morphology, head quality, and phenology (**Table 1**; **Figure 1**; Stansell et al. (2017)). LT was measured as the degree of lateral shoot growth. MH was evaluated as flower bud bunching before antithesis. MS was measured as above-ground biomass of a representative central plant. VG was evaluated as overall plant vigor. Leaf color/waxiness (LC) was evaluated visually. LA and LM were evaluated as the leaf-tip angle and degree of leaf margin serration. No intermediate flower color was detected so FC was scored as a binary trait. Other bud morphology traits (SE, SS, SF, ST, and SH) were evaluated visually as unopened buds at head maturity. The traits bud size (BS), bud uniformity (BU), bracting (BR), head compactness (HC), head diameter (HD), head uniformity (HU), head extension (HE), head shape (HS), overall-heading quality, and (OQ) were evaluated following standardized protocols developed by the Eastern Broccoli Project using an ordinal scale (1 = worst; 5 = best) with slight population specific modifications (e.g.: adjusting scale centering to account for smaller DH heads) (Stansell et al., 2017). Days to maturity and flowering (DM and DF) were calculated as days from sowing to head maturity and first flowering respectively. Holding ability HA was defined as DF–DM. Correlation matrices were computed between traits as well as between trial years by invoking the Spearman method with the cor() function in R v3.6.0 (R-Core-Team, 2018). RIA of overall heading quality OQ was conducted with the R package ratervar (Stansell et al., 2017) using 1,000 bootstraps under the metric "lmg" by fitting the model:

$$OQ \sim LT + MH + MS + VG + LA + LM + LC + BS + BU + BR + HC + HD + HE + HS + HU + DF + DM \quad (1)$$

## Marker Development, Map Construction

DNA was extracted from young leaf tissue at the 2–3 true leaf stage, bulked from five plants and extracted according to standard protocols. GBS was accomplished at the University of Wisconsin Biotechnology Center DNA Sequencing Facility following methods of Elshire et al. (2011). Library construction occurred in 96-well plates with ApeKI digestion followed by sequencing on Illumina HiSeq 2500, producing 100-bp single-end reads. SNP production was accomplished using the TASSEL v5.2.35 GBS pipeline (Glaubitz et al., 2014): 214,757,912 raw sequence reads were initially generated and 168,722,056 (78.6%) were good barcoded reads (minimum quality score > 15; minimum K-mer count = 10; min K-mer length = 10) and reads were collapsed into 11,842,938 tags. Alignment of filtered tags were was accomplished with default settings with BWA v0.7.15 (Li, 2013) to the *B. oleracea* genome v2.1 (Parkin et al., 2014), producing 670,347 mapped tags. Initial filtering removed indels, loci with more than 10% missing data and minor SNP states. Missing data were imputed using the FSFHap plugin (Swarts et al., 2014) invoking the cluster algorithm option. Nucleotide data was recoded as ABH genotypes and heterozygous, missing, or ambiguous calls were removed. Additional quality control steps using the package rqtl (v.1.44-9; Broman et al. (2003)) were performed: taxa with > 5% missing data were removed and taxa pairs exhibiting over 95% pairwise genetic similarity were pruned. Individuals exhibiting three times more crossover events above standard deviation were removed. Ultimately, 175 DH lines were included in the final datasets. Markers exhibiting identical segregation patterns were pruned. Markers with $\chi^2$ –log[p.adj] > 40 segregation were removed as likely genotyping errors. Linkage disequilibrium analysis identified 87 markers that appeared to be assigned to the wrong linkage groups and these were removed. Markers were imputed using a Viterbi algorithm and genetic maps were constructed using the Kosambi mapping function (**Supplementary Data S1–S6**).

## MQM Mapping

Multiple QTL mapping (MQM) was accomplished using rqtl using the forward and backward search algorithm stepwiseqtl() by searching for QTL models with the highest penalized LOD score (Broman et al., 2003; Arends et al., 2010). Genotypes were first simulated with hidden Markov modeling ($N$ = 1,000) followed by estimation of the true underlying genotype probabilities calculated across a 1 cm fixed stepwidths. Initially, 1,000 permutations of two-dimensional scans per trait were run to establish trait-specific genome-wide significance thresholds and to calculate MQM model penalties. An initial forward scan was used to determine the maximum number of QTL per trait to include in stepwiseqtl(). The normal model was invoked for stepwiseqtl() except for the trait FC which was run under a binary model. Between model selection steps in MQM analysis, QTL positions were refined using iterative maximum likelihood scanning. Additional non-parametric scans using extension of the Kruskal-Wallis tests were run as an additional confirmation step to account for non-normal distributions. Epistatic effects were identified using two-dimensional scans with the scantwo() function and chosen according to the $FV_1$ model: the $\log_{10}$ likelihood of the full QTL model on chromosomes $j$ and

**TABLE 1 |** Trait classes and traits evaluated within BolTBDH trials with descriptions and scoring scales.

| | Description | Range | Scale |
|---|---|---|---|
| *Architecture* | | | |
| **LT** | lateral shoot growth | 1–5 | 5 = complete absence of lateral side shoots;<br>1 = extensive side shoots |
| **MH** | head bunching | 0–1 | 1 = {HS = 2,3,4,5}; 0 = {HS = 0,1} |
| *Biomass* | | | |
| **MS** | above-ground biomass | (g) | Above ground biomass (g) |
| **VG** | plant vigor | 0–5 | 5 = the largest plants (>0.5 m to apex);<br>1 = very small plants (<0.1 m to apex);<br>0 = died in vegetative stage |
| *Leaf morphology* | | | |
| **LA** | leaf apex | 1–3 | 1 = flat; 3 = pointed |
| **LM** | leaf margin | 1–5 | 1 = completely smooth; 5 = completely serrated |
| **LC** | leaf color/waxiness | 1–3 | 1 = dark-green leaf color/low wax;<br>3 = blue-green leaf color/high wax |
| *Bud morphology* | | | |
| **FC** | flower color | 0–1 | 0 = yellow; 1 = white |
| **SE** | shape of bud ends | 1–3 | 1 = lobed; 2 = dimpled; 3 = round |
| **SF** | "fig" shaped bud ends | 0–1 | 1 = fig shaped bud; 0 = not fig shaped |
| **SH** | hooked sepals | 0–1 | 1 = "hooked" junction, 0 = smooth junction |
| **SS** | side profile of unopened flower bud | 1–3 | 1 = straight; 2 = oval; 3 = round |
| **ST** | sepal junction of unopened flower buds | 1–3 | 1 = flat junction;<br>2 = slight junction overlap;<br>3 = severe "hooked" junction |
| **BS** | bead size | 1–5 | 5 = fine beads <1.1 mm diameter,<br>3 = medium beads (1.4–1.7 mm),<br>1 = extra large beads (> 2.0 mm) |
| **BU** | bead uniformity | 1–5 | 5 = beads highly uniform across head surface;<br>3 = acceptable, but marginal uniformity of beads;<br>1 = highly variable bead size and appearance |
| *Head quality* | | | |
| **BR** | bracting | 1–5 | 5 = head entirely free of cauline leaves bisecting curd;<br>3 = moderate bisection;<br>1 = extreme leaf bisection |
| **HC** | head compaction | 1–5 | 5 = very tight floral inflorescence at head maturity;<br>1 = very loose inflorescence at head maturity |
| **HD** | head diameter | 1–5 | 5 = largest heads observed (8–10 cm across); 1 = smallest heads (2–4 cm) |
| **HE** | head extension | 1–5 | 5 = head apex is very high (e.g. >5 cm) above foliage;<br>3 = head apex at same position as top foliage;<br>1 = head apex buried deep in foliage |
| **HS** | head shape | 0–5 | 5 = convex head surface; 3 = flat surface; 0 = concave head surface |
| **HU** | head uniformity | 1–5 | 5 = very smooth, even surface across the head surface;<br>3 = acceptable uniformity across surface, moderate surface variability;<br>1 = highly distorted head surface |
| **OQ** | overall quality | 1–5 | 5 = excellent quality;<br>3 = poor quality, but recognizable as broccoli;<br>1 = not generally recognizable as broccoli with most attributes distorted |
| *Phenology* | | | |
| **DM** | days to maturity | (d) | days from sowing to head maturity |
| **DF** | days to flowering | (d) | days from sowing to flowering |
| **HA** | holding | (d) | DF – DM |

*k* was compared against a single model QTL on *j* or *k* ($p_{fv1} < 0.05$). QTL intervals were called by applying the function find_peaks() by choosing MQM peaks surpassing the genome-wide significance threshold ($\alpha = 0.05$), estimating interval start and stop locations as 95% Bayes credible intervals (BCIs), and selecting the best adjacent markers. Percent phenotypic variance explained was calculated by

$$PVE = 1 - 10^{\frac{-2^{*}LOD_{peak}}{n}} \quad (2)$$

Candidates were determined by subsetting the *B. oleracea* v2.1 genome annotation by the 95% BCI followed by further extraction of *A. thaliana* BLASTP hits. Additionally, a review of candidates implicated in developmental control of the horticultural traits under consideration was followed by pan-taxonomic searches using the online tools TAIR (Berardini et al., 2015) and EnsemblePlants (Ruffier et al., 2017) to determine the physical locations of 391 *B. oleracea* homologs (**Supplementary Data S7**). These candidates were then cross-referenced against

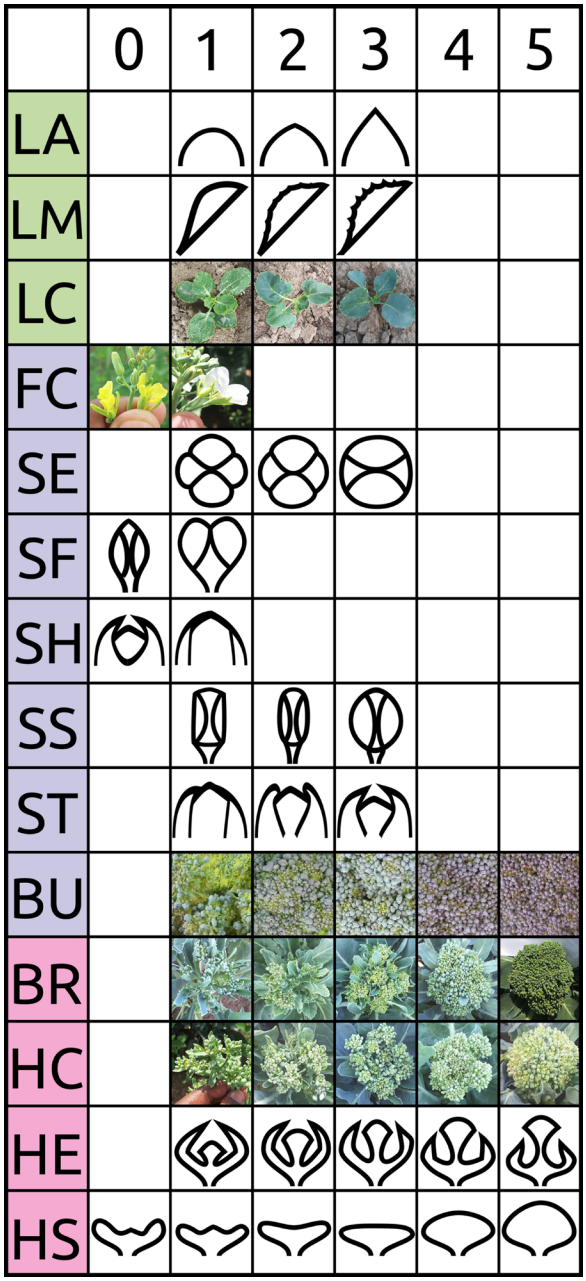


**FIGURE 1 |** Visual scoring scale of selected traits evaluated in BolTBDH trials. See **Table 1** and Stansell et al. (2017) for additional information.

the identified QTL using a custom R script that calculated the difference in physical location of a candidate and LOD peak location, retaining only candidates located within the 95% BCI or within 1 Mbp from the LOD peak.

# RESULTS

## Phenotyping

For architectural traits, suppression of lateral shoot growth (LT) was considerably higher in $Y_1$ ($Y_1$ = 3.1, $Y_2$ = 1.8; **Figure 2A**; **Table 2**) and was moderately correlated between years (r = +0.61; **Figure 2B**). Presence of floret bunching (MH) was lower in the $Y_2$ trial (0.98 vs 0.86; r = +0.22). Average above-ground biomass (MS) was 90.5 g lower in $Y_2$ trials, although plant vigor (VG) was consistent between years. MS and VG were positively correlated (r = +0.57). The leaf morphology traits LA and LM exhibited moderate between-trait correlation (r = +0.45). Leaf color (LC) was moderately correlated between years (r = +0.52). Except for flower color (FC; r = +1.00), other bud morphology traits exhibited low to intermediate year-to-year correlation, ranging from "bud profile:fig" (SF; r = +0.15) to flower bud size (BS; r = +0.55).

All head quality traits were lower in $Y_2$ when compared to $Y_1$ except for bud uniformity (BU; −0.03) and head-quality traits were strongly correlated between years (r = +0.82). Head shape (HS; −0.55) and head compactness (HC; −0.47) exhibited the largest changes from $Y_1$ to $Y_2$ trials. Overall horticultural quality (OQ) was positively correlated with all other head quality traits such as head uniformity (HU; r = +0.94) and head shape (HS; r = 0.88) except for a negative correlation with head extension HE (r = −0.51). Days to head maturity DM (r = +0.93) and flowering DF (r = +0.88) were correlated between years, although lower in $Y_2$ trials by 19.7 d and 19.4 d. DM and DF were correlated with each other (r = +0.94). Time from maturity to flowering (HA) was consistent between years ($Y_1$ = 5.34 d and $Y_2$ = 5.61 d) but was not strongly correlated with DM (r = +0.13) or DF (r = +0.39).

Relative importance analyses indicated that variation in the traits HU (24.7%), HC (21.3%), HS (16.4%), and BR (15.2%) explained 78.0% of the variability in overall heading quality model (**Figure 2C**, **Table S1**). Although OQ was correlated with DM (r = +0.53) and DF (r = 0.46), these traits were not strong predictors of OQ, each explaining < 3% of the variance in the RIA quality model.

## Genotyping and Mapping

Genotype-by-sequencing of all initial lines ($N$ = 202) resulted in 168,722,056 quality barcoded reads distributed across 2,529,429 unique tags of which 670,347 were mapped, producing 263,998 SNPs. FSFhap imputation and filtering for minor allele frequencies, missing data, and minor SNPs states reduced this value to 15,774; decreasing percent missing data from 21.0% to 2.7% (**Figure S2**). Markers assigned to the wrong linkage groups were removed (**Figure 3A**) and 1881 high-quality, non-duplicated markers were selected and distributed with a mean coverage of 4.25 SNPs/Mbp (**Table S2**).

Lines identified as hybrids indicated by heterozygous calls, twinned lines, and crossover event outliers were removed, resulting in 175 lines included in multiple QTL mapping (**Supplementary Data S1–S3**). Deviation from the expected 1:1 segregation pattern (FDR < 0.05) was observed in 61.8% of markers and 50.9% alleles were contributed from $P_1$. Several chromosomes exhibited strong segregation distortion, notably C03: 73.3% ($P_1$), C08: 67.6% ($P_2$), and C07: 63.3% ($P_1$) (**Figure 3B**). Although segregation distortion may reduce overall QTL detection power, it does not limit detection in sufficiently dense marker sets, therefore these markers were retained.

**TABLE 2 |** Phenotypic evaluations pooled across year 1 ($Y_1$) and year 2 ($Y_2$) environments ± sd; $Y_1$ and $Y_2$ means ±sd; (ρ) = Spearman correlations between $Y_1$ and $Y_2$ evaluations.

| | Scale | $Y_{12}$ | $Y_1$ | $Y_2$ | ρ |
|---|---|---|---|---|---|
| *Architecture* | | | | | |
| **LT** | 1–5 | 2.44 ± 0.67 | 3.09 ± 0.92 | 1.80 ± 0.54 | +0.61 |
| **MH** | 0–1 | 0.92 ± 0.18 | 0.98 ± 0.11 | 0.86 ± 0.29 | +0.22 |
| *Biomass* | | | | | |
| **MS** | (g) | 415 ± 105 | 447 ± 118 | 356 ± 115 | +0.51 |
| **VG** | 1–5 | 2.67 ± 0.57 | 2.64 ± 0.6 | 2.71 ± 0.61 | +0.72 |
| *Leaf Morphology* | | | | | |
| **LA** | 1–3 | 2.23 ± 0.38 | 2.16 ± 0.39 | 2.30 ± 0.45 | +0.59 |
| **LM** | 1–5 | 2.66 ± 0.55 | 2.78 ± 0.66 | 2.63 ± 0.57 | +0.67 |
| **LC** | 1–3 | 2.06 ± 0.39 | 1.96 ± 0.31 | 2.15 ± 0.57 | +0.52 |
| *Bud Morphology* | | | | | |
| **FC** | 0–1 | 0.77 ± 0.42 | 0.78 ± 0.42 | 0.77 ± 0.42 | +1.00 |
| **SE** | 1–3 | 1.82 ± 0.49 | 1.85 ± 0.57 | 1.75 ± 0.62 | +0.38 |
| **SF** | 0–1 | 0.13 ± 0.21 | 0.17 ± 0.26 | 0.08 ± 0.26 | +0.15 |
| **SH** | 0–1 | 0.20 ± 0.26 | 0.24 ± 0.30 | 0.10 ± 0.29 | +0.24 |
| **SS** | 1–3 | 2.28 ± 0.44 | 2.21 ± 0.49 | 2.41 ± 0.56 | +0.30 |
| **ST** | 1–3 | 2.23 ± 0.50 | 2.19 ± 0.58 | 2.34 ± 0.62 | +0.26 |
| **BS** | 1–5 | 2.87 ± 0.57 | 2.84 ± 0.66 | 2.90 ± 0.62 | +0.55 |
| **BU** | 1–5 | 3.48 ± 0.41 | 3.46 ± 0.51 | 3.49 ± 0.52 | +0.24 |
| *Head Quality* | | | | | |
| **BR** | 1–5 | 3.43 ± 0.88 | 3.56 ± 1.01 | 3.28 ± 0.88 | +0.70 |
| **HC** | 1–5 | 2.96 ± 0.82 | 3.19 ± 0.80 | 2.72 ± 0.92 | +0.78 |
| **HD** | 1–5 | 2.55 ± 0.73 | 2.64 ± 0.86 | 2.45 ± 0.73 | +0.58 |
| **HE** | 1–5 | 2.91 ± 0.68 | 2.95 ± 0.75 | 2.84 ± 0.70 | +0.73 |
| **HS** | 1–5 | 2.72 ± 0.91 | 3.01 ± 0.89 | 2.46 ± 1.04 | +0.73 |
| **HU** | 1–5 | 2.77 ± 0.72 | 2.87 ± 0.74 | 2.68 ± 0.79 | +0.73 |
| **OQ** | 1–5 | 2.72 ± 0.80 | 2.80 ± 0.87 | 2.63 ± 0.79 | +0.83 |
| *Phenology* | | | | | |
| **DM** | (d) | 76.6 ± 7.7 | 86.3 ± 7.2 | 66.6 ± 7.8 | +0.93 |
| **DF** | (d) | 81.6 ± 7.4 | 91.3 ± 6.8 | 71.9 ± 8.3 | +0.88 |
| **HA** | (d) | 5.45 ± 2.3 | 5.3 ± 1.9 | 5.6 ± 3.3 | +0.51 |

A genetic map was constructed from 1,881 markers spanning all linkage groups (**Figures 3A–C**), with markers per chromosome ranging from 106 (C01) to 283 (C03). Total map distance was 1,060.8 cm with a mean and maximum marker spacing of 0.57 and 16.67 cm/marker. Maximum marker spacing per chromosome ranged from 2.26 cm/marker (C08) to 16.67 cm/marker (C05). Mean crossover events per double haploid were 15.0 ± 9.7; max = 61, min = 4.

## MQM Mapping

MQM identified 56 single (**Figure 4A**; **Table 3**) and 41 epistatic (**Table 5**; **Figure 5**) QTL. QTL per chromosome ranged from 1 (C02) to 12 (C09)(**Figure 4B**). LOD values ranged from 2.85 (MS_C05@39.5; PVE = 7.3) to 39.9 (FC_C03@55.7; PVE = 65.8). Bayesian confidence intervals (95% CI) ranged from 0.3 to 59.9 Mbp (mean = 16.2 Mbp), and contained on average 1902.2 coding sequences and 330.6 A. *thaliana* hits (**Table 4**). QTL per trait class ranged from 3 (biomass) to 20 (head quality). Three architecture trait QTL were identified for LT, and no MH QTL were identified. Four biomass QTL were identified, one MS and three VG. Nine leaf morphology QTL were identified: five LA, three LM, and one LC. Thirteen significant bud morphology QTL were identified: one FC, SE, SF, SH, SS, and ST, five BS, and two BU. Twenty head quality QTL were identified, including two BR, two HC, three HD, three HE, two HS, three HU, and four OQ. Seven phenology QTL were identified: two DM, two DF, and three HA. Epistatic QTL ($p < 0.05$) were detected in every trait class except FC, MH, and SS.

Optimal MQM models were determined for all traits ranging in complexity from FC: FC ~ 3@55.7 to LA ~ 1@3.4 + 3@0.7 + 6@18.7 + 7@37.0 + [3@0.0 × 9@48.5] + [3@0.0 × 7@36.6] + [7@36.9 x 9@24.4] + [1@2.6 x 9@49.5] + [6@18.7 × 7@36.7] + [1@2.6 × 3@0.0] + [2@3.1 × 8.5] (**Table 5**).

Ten QTL hotspots appearing to harbor QTL across multiple traits were identified: two biomass related ($Bio_5$ and $Bio_7$), four morphology related ($Bud_1$, $Lea_3$, $Bud_4$, and $Lea_7$), three heading quality related ($HQ_4$, $HQ_8$, and $HQ_9$), and one phenology related ($Phe_3$) (**Table 4**).

# DISCUSSION

## Phenotyping

Field evaluations were conducted in growing seasons that differed somewhat in temperature stress (**Figure S1**). In year two ($Y_2$), a strong heat wave in the first half of July (mean high = 29.5°C) coincided with the reproductive transition. Horticultural quality scores were lower in $Y_2$ trails, likely due to less optimal temperatures during the transition to flowering (**Table 2**) [e.g.:

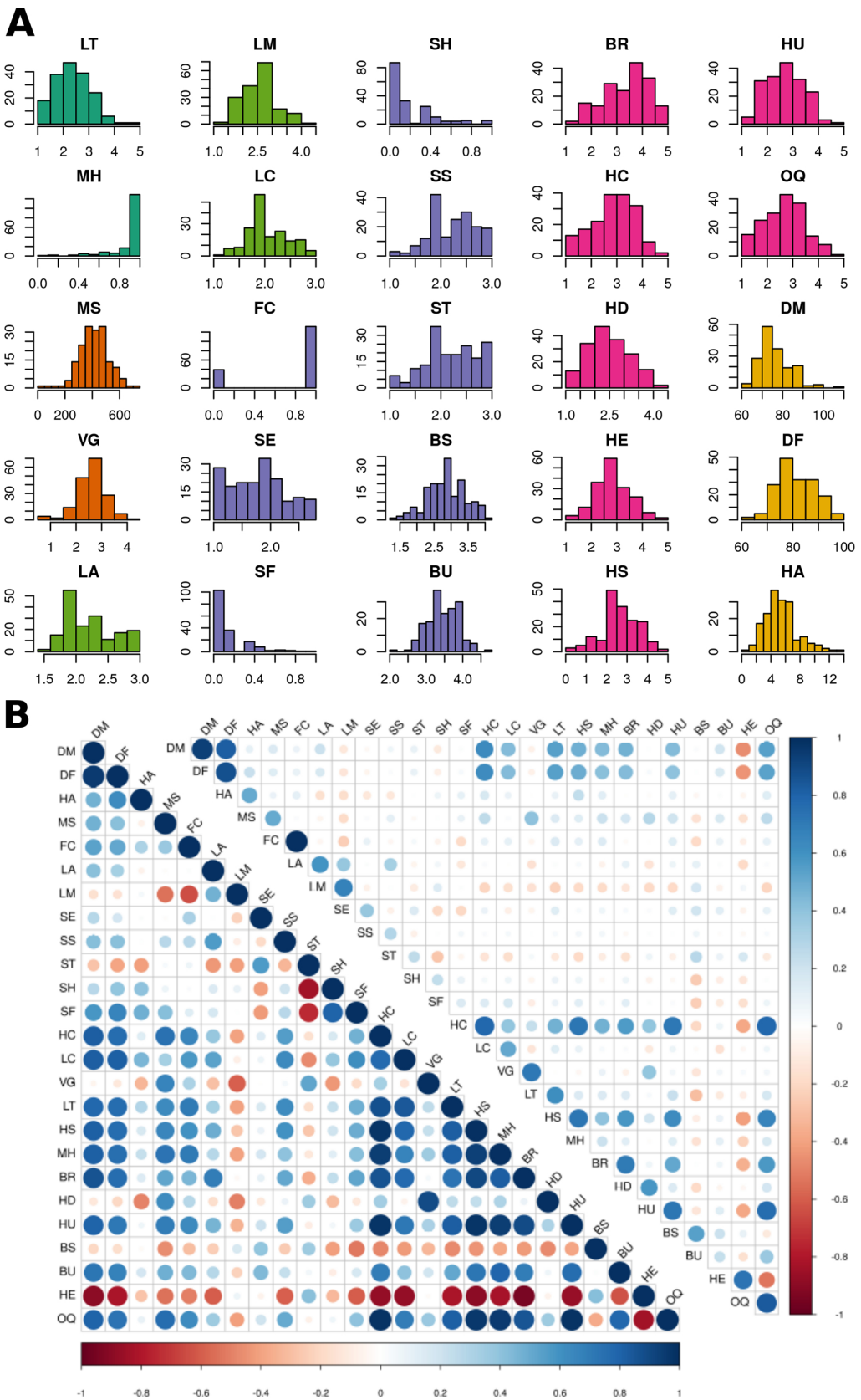


**FIGURE 2 |** Continued

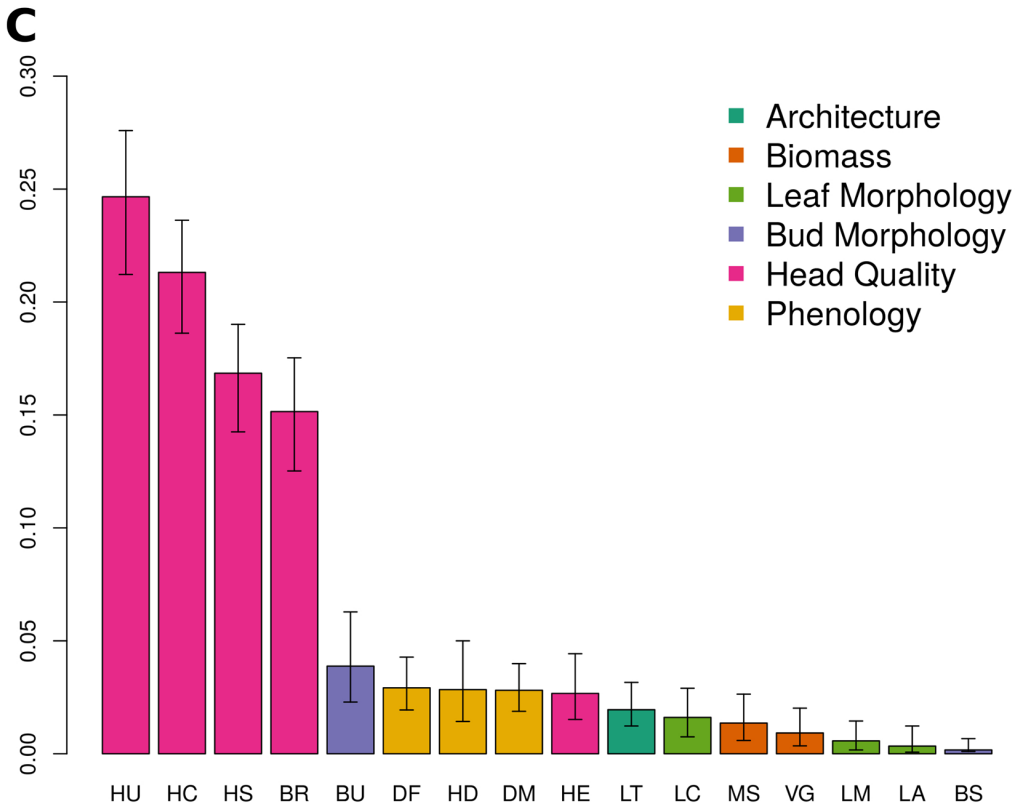


**FIGURE 2 |** BolTBDH phenotypic analysis: **(A)** Distribution of phenotypic traits evaluated in year 1 and year 2 ($Y_{12}$) trials. Trait class is indicated by color (architecture = dark green, biomass = orange, leaf morphology = light green, bud morphology = light blue, heading quality = pink, and phenology = yellow). **(B)** $Y_{12}$ between-trait (bottom left) and between-year $Y_1$ vs. $Y_2$ (top right) Spearman correlation coefficients, with negative and positive correlations plotted in red and blue. **(C)** Percentage of $Y_{12}$ overall quality model explained by relative importance predictors (RIA) by fitting the model [*OQ ~ LT + MH + MS + VG + LA + LM + LC + BS + BU + BR + HC + HD + HE + HS + HU + DF + DM*] using the lmg method with the rateRvaR function raterimp() with 95% confidence intervals estimated by 1,000 permutations.

suppression of lateral shoot growth (LT) was evaluated 1.3 points lower in $Y_2$ trials].

## Genotyping and Mapping

The GBS markers (**Figure 3A** and **Figure S2**) generated were high quality with less than 5% missing data and distributed across all chromosomes with a mean coverage 1.77 markers/cM (**Figure 3C**; **Table S2**; **Figure S3**), a six-fold improvement in marker coverage from previous BolTBDH maps, which relied upon approximately 300 SSR and RFLP markers (Sotelo Pérez et al., 2014; Francisco et al., 2016). Segregation distortion was prevalent but chromosome-specific (C03, C07, C08; **Figure 3B**).

## MQM Analysis

### Architecture

Excessive lateral side-shoot growth is a horticultural defect that increases harvest costs and reduces yield. Although improved broccoli $F_1$ hybrids typically exhibit strong apical dominance, variability in lateral side-shoot growth occurs among genotypes, typically under environmentally stressed conditions (Potters et al., 2007). In a bulk-segregant analysis of shoot branching in *B. juncea*, Muntha et al. (2018) identified *BjPAT1* and its signal integrator *BjBRC1* as branching candidates. The *BoPAT1* or *BoBRC1* homologs did not collocate with the LT BCI identified in BolTBDH. Tyagi et al. (2019) determined that mutations in *BjSOC1* may influence degree of lateral branching. A *BoSOC1* ortholog (Bo3g038880) was identified within the 95% LT_C03@5.9 BCI, although this candidate was located >9.5 Mbp from the LOD peak, and is not likely involved in the LT phenotype response observed in BolTBDH. He et al. (2017) conducted GWA and QTL mapping of lateral branching in *B. napus* and identified *BnaC03g63480D* as a branching number candidate. The best *BnaC03g63480D* ortholog, Bo3g159770, was nominally located within the LT_C03@5.9 BCI, but is not considered a likely candidate within this population. Additional candidates associated with meristem identity and fate identified within LT QTL are listed (**Table 6**).

### Biomass

In broccoli, higher yielding genotypes are preferred for commercial production and vegetative biomass is positively correlated with head biomass (Lin et al., 2013). In a $F_2$ broccoli ×

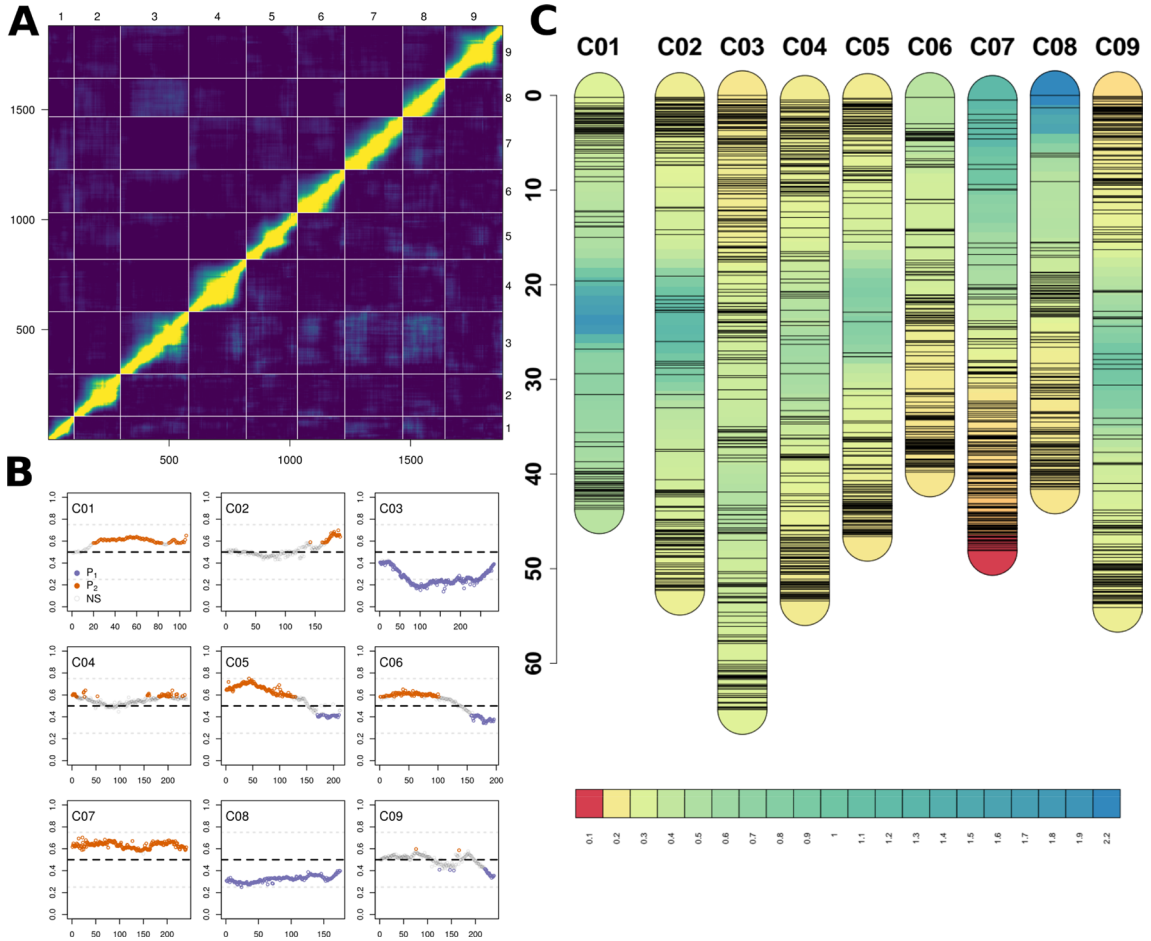


**FIGURE 3 | (A)** Heatmap of relative recombination fractions (top left) and logarithm of odds scores (bottom right) comparing all pairs of the 1,881 markers (bottom and left axes) and by chromosome (top and right axes) used to construct BolTBDH genetic map. **(B)** Segregation distortion (Y-axis; $f = P_1$ allele) observed using all markers (X-axis) disaggregatted by chromosomes (C01–C09). Markers exhibiting significant segregation distortion ($\chi^2$ [p.adj] < 0.05) plotted in orange ($P_1$) or purple ($P_2$). Non-significant segregation distortion markers are plotted in grey. **(C)** Genetic map, marker location (cm), and marker density (cm/marker) by chromosome using all 1,881 BolTBDH markers.

broccoli population, Lin et al. (2013) identified biomass QTL on linkage groups C1, C5, C8, and C9, although the authors did not identify candidates associated with these loci. In a GWA study of seedling vigor in *B. napus*, the vigor candidates *Bna.SCO1*, *Bna.ARR4*, and *Bna.ATE1* were identified by Hatzig et al. (2015), although no homologous candidates were located within the BolTBDH VG BCIs. A GWA and transcriptome analysis in *B. napus* by Lu et al. (2017) identified two yield-related candidates: *BnaA05g29680D* and *BnaC04g42030D*. These candidates were not identified in BolTBDH biomass QTL, although one ortholog of *BnaA05g29680D* (Bo5g139830) was identified adjacent to the $Bio_5$ hotspot.

The homologous candidates *BRC1* (Bo1g117490 and Bo5g117410) is closely related to *TEOSINTE BRANCHED1*, and is a putative transcription factor involved in arresting axillary bud development and limiting axillary bud growth (Muntha et al., 2018) and was identified within $Bio_5$. Additional homologous VG candidates involved in growth and growth regulation were identified (**Table 6**).

## Leaf Morphology

Variation in leaf morphology is useful to improve and develop novel market classes of *B. oleracea* leafy greens. Lan and Paterson (2000) identified robust QTL associated with leaf lamina width on C01 and C07, although they did not identify likely candidates. Previous studies have identified leaf-apex QTL on LGO1 and LGO3 (cauliflower × Brussels sprouts) (Sebastian et al., 2002) and C06 and C07 (broccoli × broccoli) (Walley et al., 2012). Li et al. (2009) identified the candidate *BrAS1* involved in leaf lamina width. The candidates *AtLUG*, *AtWOX1*, and *AtAN3* were shown by Zhang et al. (2019) to be involved in leaf blade outgrowth although none of these candidates were identified in LA BCI within BolTBDH. In *Arabidopsis*, *gif1* mutants exhibit a longer, narrow leaf phenotype (Shimano et al., 2018) and a *GIF1* homolog (Bo7g093130) collocated within LA_C07@36.6 QTL.

In a QTL-seq analysis of ornamental kale, Ren et al. (2019) identified a lobed-leaf candidate *BoLl* to C09 (38.82–40.12 Mb), although *BoLl* did not collocate with BolTBDH LM QTL. Ni et al. (2017) transformed *BnLMI1* into *Arabidopsis* producing serrated

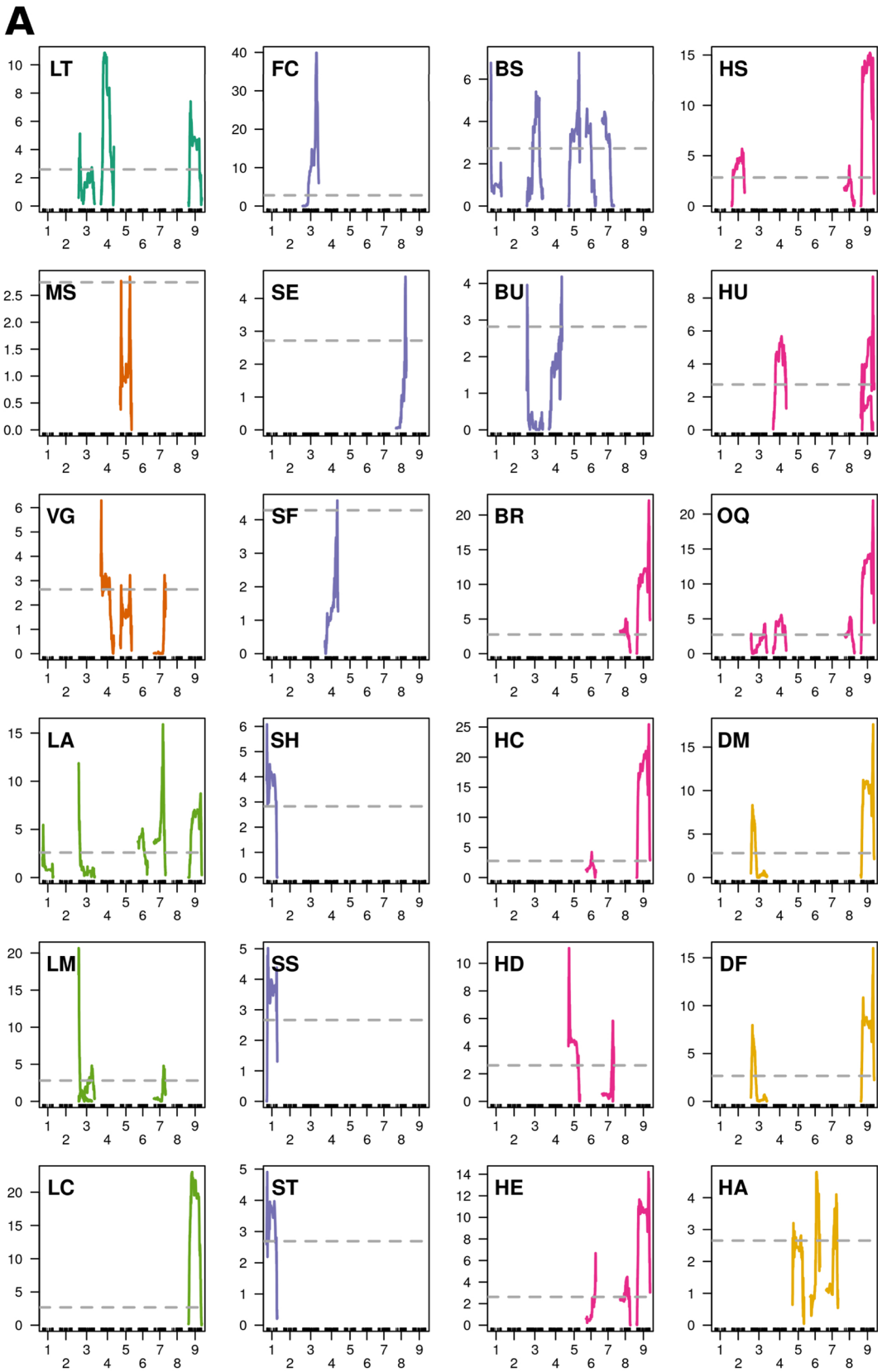


**FIGURE 4 |** Continued

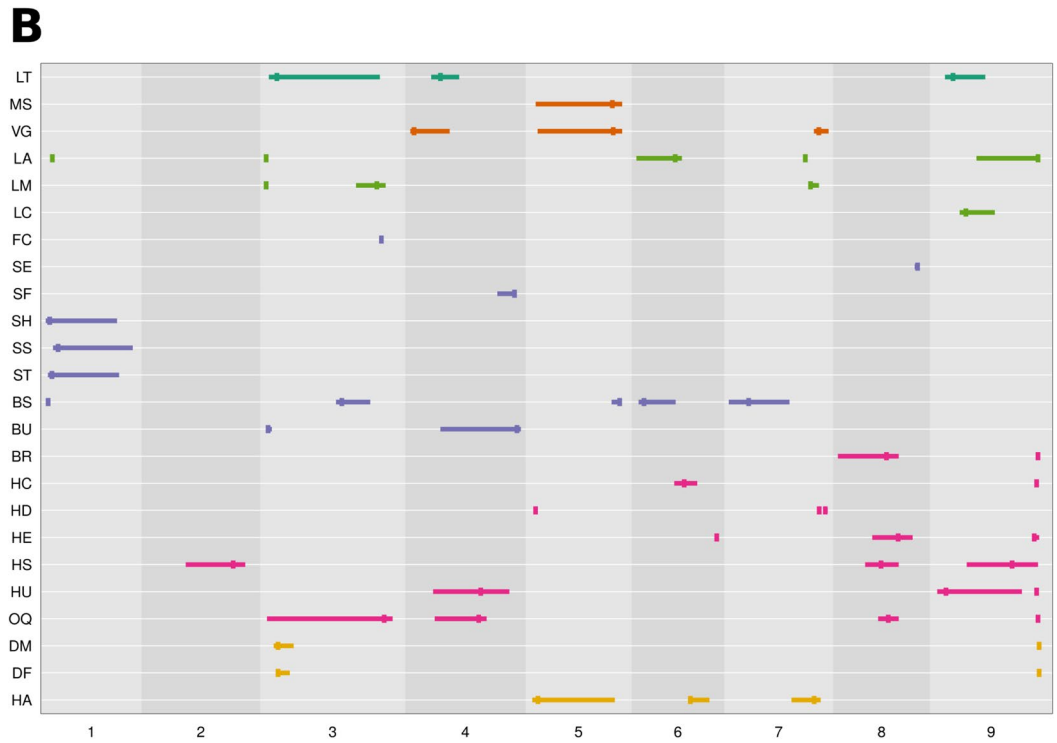


**FIGURE 4 |** MQM QTL mapping results: **(A)** QTL plots by trait and chromosome using 1881 markers, 175 double haploid lines, and pooled phenotypes across environments ($Y_{12}$; X-axis = chromosome, Y-axis = LOD). Horizontal, dashed, grey line = genome-wide significance threshold ($\alpha = 0.95$) determined from 1,000 permutations of scantwo() for individual traits. Trait class is indicated by color (architecture = dark green, biomass = orange, leaf morphology = light green, bud morphology = light blue, heading quality = pink, and phenology = yellow). **(B)** Summarized MQM results; traits evaluated in BolTBDH printed along the Y-axis and chromosomes scaled by physical distance (Mbp) are arranged on the X-axis. MQM peak apex given by vertical bar and 95% Bayesian confidence intervals indicated by width of horizontal bar. Color schema is recycled from **(A)**.

leaf margins, similar in appearance to the serrated leaf margin phenotype observed in BolTBDH. In BolTBDH, a *BoLMI1* ortholog (Bo3g002560) collocated closely with $Lea_3$ in agreement with Ni et al. (2017).

Alterations in cuticular wax alters herbivore behavior and may confer broad resistance (Branham and Farnham, 2017). Leaf color in *B. oleracea* is strongly affected by cuticle wax content and is likely responsible for the variation in blue-green matte and dark-green glossy leaf appearance observed in the BolTBDH population. Xu et al. (2019) conducted fine mapping of the cuticular wax synthesis gene *BoWax1* controlling the glossy trait in a $F_2$ cabbage population although this candidate was not identified in BolTBDH LC BCI. In another cabbage population segregating for the glossy leaves, Zhu et al. (2019) mapped a non-wax glossy *NWGL* locus to a 99 kb interval in C08. Neither *BoWax1* or the *NWGL* locus collocated with the LC QTL identified in BolTBDH. Lee et al. (2015b) analyzed expression of wax synthesis candidates and determined that the homologous candidates *LACS1*, *KCS1*, *KCR1*, *ECR*, *CER3*, and *MAH1* were differentially expressed in broccoli lines with elevated cuticular wax levels. Of these candidates, only *MAH1* homologs collocated with LC_C09@15.1 and the BCI included five *MAH1* copies: Bo9g053360, Bo9g053340, Bo9g053260, Bo9g053220, Bo9g053170. *MAH1* encodes CYP96A15, a midchain alkane hydroxylase, involved in cuticular wax biosynthesis (Greer et al., 2007).

## Bud Morphology

*B. oleracea* flower petals are typically white, but a dominant mutation of *BoCCD4* implicated in a yellow-flower phenotype *via* inactivation of a carotenoid-degrading enzyme has been previously described (Zhang et al., 2015; Han et al., 2019). In BolTBDH, a single flower color QTL was identified (FC_C03@55.7) and *BoCCD4* (Bo3g158650; C03:56.61Mb) was located < 1 Mbp from this LOD peak, in agreement with (Zhang et al., 2015). Interestingly, 77.2% of BolTBDH lines exhibited a white flower phenotype, an unexpected result given single locus control in the MQM trait model FC ~ 3@55.7, however the segregation distortion observed at this locus ($f = 0.76$ $P_1$) is consistent with this result (**Figure 3B**).

Certain bud morphology defects contribute to a reduction in head quality, often rendering broccoli heads unmarketable. Hooked sepals are commonly encountered in broccoli hybrids, resulting in a non-uniform crown surface and a reduced ability to shed water. In *B. rapa*, Zhang et al. (2018) identified loss-of-function *BrAP2* alleles with sepal defects similar to the hooked sepal phenotype observed in BolTBDH. In BolTBDH, the optimal MQM model for hooked sepals (SH ~ 1@2.1 + [1@0.2

**TABLE 3 |** Multiple mapping QTL identified in pooled $Y_{12}$ dataset for individual traits (**Trait**) within trait classes.

| | Trait | CHR | LOD | POS | $ci_{low}$ | $ci_{high}$ | MAR* | PVE | P1 | P2 | Δ |
|---|---|---|---|---|---|---|---|---|---|---|---|
| *Architecture* | | | | | | | | | | | |
| LT_C03@5.9 | LT | 3 | 5.1 | 5.9 | 2.0 | 55.0 | SC3_5860860 | 12.69 | 2.64 | 2.37 | +0.27 |
| LT_C04@15.0 | LT | 4 | 10.8 | 15.0 | 10.6 | 23.9 | SC4_15017345 | 24.96 | 2.68 | 2.17 | +0.51 |
| LT_C09@9.0 | LT | 9 | 7.4 | 9.0 | 5.1 | 24.4 | SC9_8986159 | 17.81 | 2.66 | 2.19 | +0.47 |
| *Biomass* | | | | | | | | | | | |
| MS_C05@39.5 | MS | 5 | 2.8 | 39.5 | 2.9 | 44.2 | SC5_39489450 | 7.26 | 390.38 | 447.64 | –57.26 |
| VG_C04@2.4 | VG | 4 | 6.3 | 2.4 | 0.7 | 19.4 | SC4_2430671 | 15.34 | 2.86 | 2.42 | +0.44 |
| VG_C05@39.9 | VG | 5 | 3.2 | 39.9 | 3.9 | 44.2 | SC5_39919197 | 8.18 | 2.54 | 2.84 | –0.30 |
| VG_C07@43.4 | VG | 7 | 3.2 | 43.4 | 41.0 | 48.0 | SC7_43403602 | 8.19 | 2.80 | 2.49 | +0.30 |
| *Leaf Morphology* | | | | | | | | | | | |
| LA_C01@3.4 | LA | 1 | 5.5 | 3.4 | 3.0 | 3.9 | SC1_3378511 | 13.46 | 2.15 | 2.36 | –0.21 |
| LA_C03@0.7 | LA | 3 | 11.9 | 0.7 | 0.0 | 1.0 | SC3_722361 | 26.94 | 2.05 | 2.35 | –0.31 |
| LA_C06@18.7 | LA | 6 | 5.1 | 18.7 | 0.2 | 21.9 | SC6_18698210 | 12.57 | 2.15 | 2.35 | –0.20 |
| LA_C07@37.0 | LA | 7 | 15.9 | 37.0 | 36.5 | 37.1 | SC7_36965391 | 34.36 | 2.10 | 2.46 | –0.37 |
| LA_C09@49.5 | LA | 9 | 8.7 | 49.5 | 20.1 | 50.1 | SC9_49495162 | 20.61 | 2.34 | 2.10 | +0.24 |
| LM_C03@0.7 | LM | 3 | 20.6 | 0.7 | 0.5 | 1.3 | SC3_722361 | 42.10 | 2.25 | 2.94 | –0.69 |
| LM_C03@53.5 | LM | 3 | 4.8 | 53.5 | 43.6 | 57.7 | SC3_53485976 | 11.96 | 2.90 | 2.58 | +0.32 |
| LM_C07@39.5 | LM | 7 | 4.8 | 39.5 | 38.9 | 43.5 | SC7_39439192 | 11.90 | 2.53 | 2.87 | –0.34 |
| LC_C09@15.1 | LC | 9 | 23.0 | 15.1 | 12.1 | 28.9 | SC9_15164371 | 45.64 | 2.34 | 1.82 | +0.53 |
| *Bud Morphology* | | | | | | | | | | | |
| FC_C03@55.7 | FC | 3 | 39.9 | 55.7 | 55.7 | 56.1 | SC3_55671967 | 65.83 | 0.00 | 1.00 | –1.00 |
| SE_C08@38.0 | SE | 8 | 4.7 | 38.0 | 36.6 | 38.9 | SC8_38021928 | 11.61 | 2.04 | 1.69 | +0.35 |
| SF_C04@50.3 | SF | 4 | 4.6 | 50.3 | 42.1 | 51.3 | SC4_50348003 | 11.40 | 0.08 | 0.22 | –0.14 |
| SH_C01@2.1 | SH | 1 | 6.1 | 2.1 | 0.2 | 34.2 | SC1_2101416 | 14.86 | 0.10 | 0.30 | –0.20 |
| SS_C01@6.1 | SS | 1 | 5.0 | 6.1 | 3.7 | 41.7 | SC1_6098441 | 12.50 | 2.16 | 2.48 | –0.32 |
| ST_C01@3.2 | ST | 1 | 4.9 | 3.2 | 1.3 | 35.2 | SC1_3205069 | 12.18 | 2.37 | 2.02 | +0.36 |
| BS_C01@1.3 | BS | 1 | 6.8 | 1.3 | 0.8 | 1.9 | SC1_1324660 | 16.49 | 3.06 | 2.67 | +0.39 |
| BS_C03@36.8 | BS | 3 | 5.4 | 36.8 | 34.0 | 50.3 | SC3_36786929 | 13.40 | 3.13 | 2.78 | +0.36 |
| BS_C05@43.0 | BS | 5 | 7.2 | 43.0 | 39.1 | 43.4 | SC5_42975016 | 17.53 | 3.04 | 2.69 | +0.35 |
| BS_C06@3.8 | BS | 6 | 4.6 | 3.8 | 1.2 | 18.9 | SC6_3829212 | 11.53 | 2.74 | 3.04 | –0.30 |
| BS_C07@9.9 | BS | 7 | 4.5 | 9.9 | 0.5 | 29.4 | SC7_9938249 | 11.18 | 3.00 | 2.65 | +0.35 |
| BU_C03@1.7 | BU | 3 | 4.0 | 1.7 | 1.3 | 3.4 | SC3_1653377 | 10.00 | 3.63 | 3.37 | +0.25 |
| BU_C04@51.5 | BU | 4 | 4.2 | 51.5 | 15.0 | 53.4 | SC4_51533618 | 10.54 | 3.59 | 3.33 | +0.26 |
| *Head Quality* | | | | | | | | | | | |
| BR_C08@23.2 | BR | 8 | 5.0 | 23.2 | 0.0 | 29.0 | SC8_23202902 | 12.54 | 3.82 | 3.24 | +0.57 |
| BR_C09@49.5 | BR | 9 | 22.1 | 49.5 | 48.8 | 49.6 | SC9_49467903 | 44.46 | 3.95 | 2.82 | +1.14 |
| HC_C06@23.0 | HC | 6 | 4.2 | 23.0 | 18.2 | 29.2 | SC6_23004082 | 10.66 | 3.11 | 2.71 | +0.41 |
| HC_C09@48.8 | HC | 9 | 25.4 | 48.8 | 48.8 | 49.5 | SC9_48825632 | 49.19 | 3.48 | 2.37 | +1.12 |
| HD_C05@2.9 | HD | 5 | 11.1 | 2.9 | 2.6 | 3.3 | SC5_2892857 | 25.57 | 2.40 | 2.88 | –0.48 |
| HD_C07@43.6 | HD | 7 | 5.8 | 43.6 | 43.1 | 44.5 | SC7_43553366 | 14.39 | 2.70 | 2.25 | +0.45 |
| HD_C07@46.5 | HD | 7 | 3.9 | 46.5 | 46.4 | 47.6 | SC7_46405906 | 9.97 | 2.72 | 2.24 | +0.47 |
| HE_C06@38.5 | HE | 6 | 6.7 | 38.5 | 38.2 | 38.9 | SC6_38501911 | 16.28 | 3.12 | 2.78 | +0.35 |
| HE_C08@28.8 | HE | 8 | 4.5 | 28.8 | 16.4 | 35.7 | SC8_28751686 | 11.24 | 2.60 | 3.04 | –0.44 |
| HE_C09@47.7 | HE | 9 | 14.2 | 47.7 | 47.1 | 50.1 | SC9_47686952 | 31.48 | 2.57 | 3.23 | –0.66 |
| HS_C02@41.7 | HS | 2 | 5.7 | 41.7 | 19.1 | 47.5 | SC2_41701063 | 14.05 | 3.00 | 2.44 | +0.57 |
| HS_C08@20.6 | HS | 8 | 4.0 | 20.6 | 13.0 | 29.0 | SC8_20577182 | 10.11 | 3.17 | 2.54 | +0.63 |
| HS_C09@37.1 | HS | 9 | 15.2 | 37.1 | 15.5 | 49.5 | SC9_37685257 | 33.30 | 3.27 | 2.27 | +1.01 |
| HU_C04@34.2 | HU | 4 | 5.7 | 34.2 | 11.5 | 47.9 | SC4_34234727 | 14.03 | 2.98 | 2.52 | +0.47 |
| HU_C09@5.6 | HU | 9 | 4.0 | 5.6 | 1.4 | 41.8 | SC9_5621807 | 10.03 | 3.08 | 2.34 | +0.74 |
| HU_C09@48.8 | HU | 9 | 9.3 | 48.8 | 48.8 | 49.5 | SC9_48825632 | 21.92 | 3.19 | 2.30 | +0.89 |
| OQ_C03@57.0 | OQ | 3 | 4.3 | 57.0 | 1.1 | 61.0 | SC3_56998411 | 10.79 | 2.47 | 2.78 | –0.32 |
| OQ_C04@33.3 | OQ | 4 | 5.5 | 33.3 | 12.3 | 37.0 | SC4_33280409 | 13.73 | 2.95 | 2.43 | +0.51 |
| OQ_C08@24.0 | OQ | 8 | 5.3 | 24.0 | 19.2 | 29.0 | SC8_23363239 | 13.08 | 3.04 | 2.56 | +0.48 |
| OQ_C09@49.5 | OQ | 9 | 21.9 | 49.5 | 48.8 | 49.5 | SC9_49484618 | 44.24 | 3.17 | 2.17 | +1.00 |
| *Phenology* | | | | | | | | | | | |
| DM_C03@6.4 | DM | 3 | 8.3 | 6.4 | 4.3 | 13.9 | SC3_6383243 | 19.87 | 81.96 | 74.71 | +7.25 |
| DM_C09@50.0 | DM | 9 | 17.6 | 50.0 | 49.5 | 50.1 | SC9_50021553 | 37.42 | 80.46 | 71.62 | +8.84 |
| DF_C03@6.4 | DF | 3 | 8.0 | 6.4 | 5.5 | 12 | SC3_6383243 | 19.2 | 86.78 | 79.81 | +6.97 |
| DF_C09@50.0 | DF | 9 | 16.0 | 50.0 | 50.0 | 50.1 | SC9_50021553 | 34.84 | 85.22 | 76.97 | +8.26 |
| HA_C05@4.0 | HA | 5 | 3.2 | 4.0 | 1.3 | 40.7 | SC5_4028759 | 8.22 | 5.89 | 4.65 | +1.24 |
| HA_C06@25.9 | HA | 6 | 4.8 | 25.9 | 24.8 | 35.0 | SC6_25942835 | 12.07 | 6.11 | 4.53 | +1.58 |
| HA_C07@41.2 | HA | 7 | 4.1 | 41.2 | 30.4 | 44.3 | SC7_41180016 | 10.40 | 6.04 | 4.68 | +1.36 |

*Chromosome (**CHR**), logarithm of odds (**LOD**), and physical position (**POS**; Mbp) of peak maxima with lower ($ci_{low}$) and upper ($ci_{low}$) bounds of 95% Bayesian confidence intervals.*

*The best SNP marker (**MAR***) for a given QTL and percent phenotypic variance explained (**PVE**) by QTL as calculated by $PVE = 1–10^{\frac{-2*LOD_{peak}}{n}}$ is given. Parental means for "TO1000" ($P_1$) and "Early Big" ($P_2$), with QTL effects as ($\Delta$) = $P_2–P_1$.*

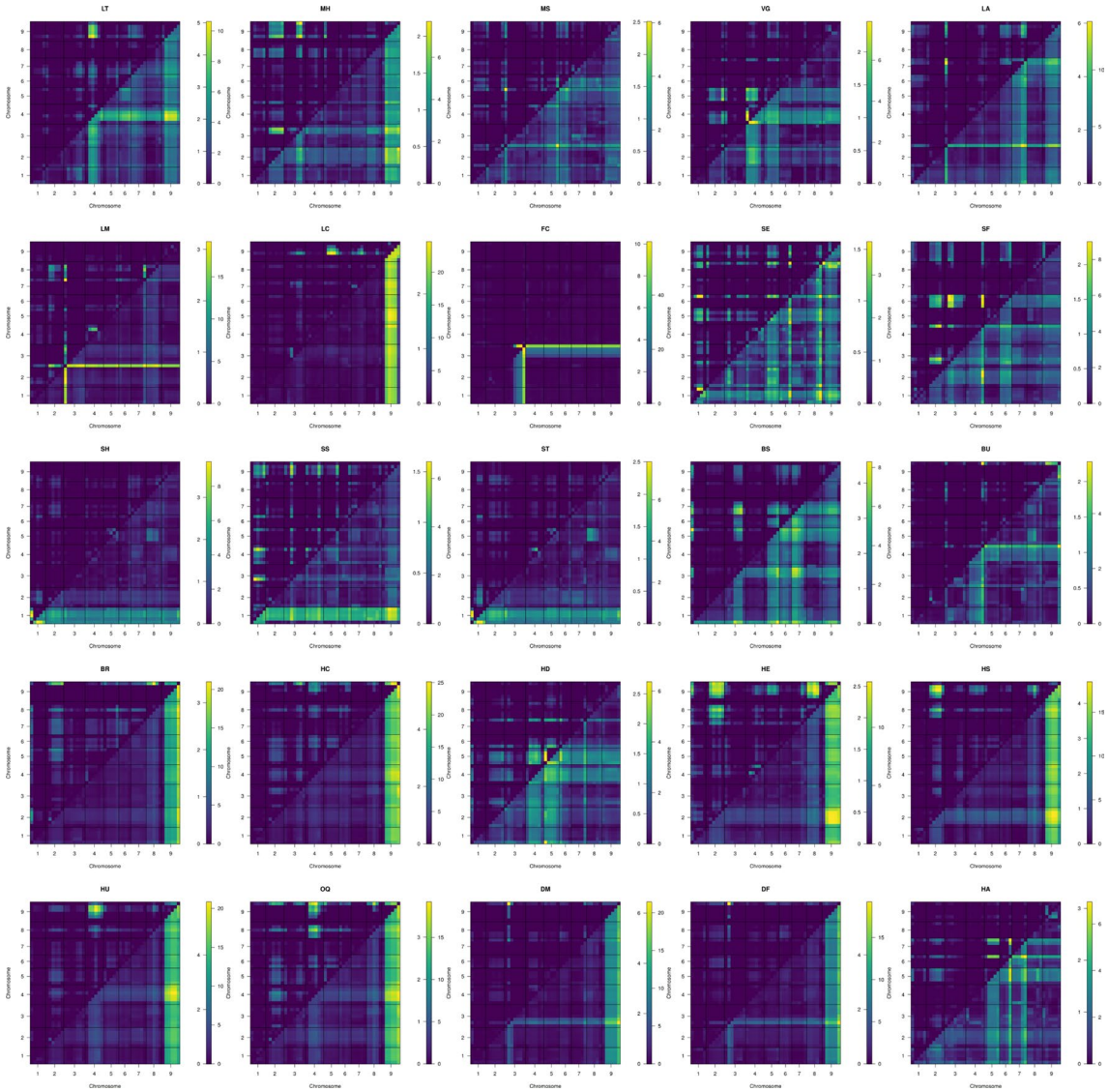


**FIGURE 5 |** Two dimensional scans of all traits using 1,881 markers, using simulated genotype probabilities (*N* = 1000) with genotype probabilities calculated across 1 cm steps. Epistatic LOD scores are calculated the difference in the log-likelihood of the full model and the additive model for a given QTL pair and are printed above and left of trace. The full model LOD values are printed below and right of trace.

**TABLE 4 |** Key genomic regions (**hotspot**) associated with multiple traits within BolTBDH multiple QTL mapping, identified by chromosome (**chr**), and interval (**start** and **stop**; Mbp) and single trait QTL identified within the interval.

| Hotspot | chr | start | stop | QTL |
|---|---|---|---|---|
| **$Bud_1$** | 1 | 1.3 | 6.1 | BS_C01@1.3, SH_C01@2.1, ST_C01@3.2, LA_C01@3.4, SS_C01@6.1 |
| **$Lea_3$** | 3 | 0.7 | 1.7 | LA_C03@0.7, LM_C03@0.7, BU_C03@1.7 |
| **$Phe_3$** | 3 | 6.4 | 6.4 | DM_C03@6.4, DF_C03@6.4 |
| **$HQ_4$** | 4 | 33.3 | 34.2 | OQ_C04@33.3, HU_C04@34.2 |
| **$Bud_4$** | 4 | 50.3 | 51.5 | SF_C04@50.3, BU_C04@51.5 |
| **$Bio_5$** | 5 | 39.5 | 39.9 | MS_C05@39.5, VG_C05@39.9 |
| **$Lea_7$** | 7 | 37.0 | 39.5 | LA_C07@37.0, LM_C07@39.5 |
| **$Bio_7$** | 7 | 43.4 | 43.6 | VG_C07@43.4, HD_C07@43.6 |
| **$HQ_8$** | 8 | 20.6 | 28.8 | HS_C08@20.6, BR_C08@23.2, OQ_C08@24.0, HE_C08@28.8 |
| **$HQ_9$** | 9 | 47.7 | 50.0 | HE_C09@47.7, HC_C09@48.8, HU_C09@48.8, LA_C09@49.5, BR_C09@49.5, OQ_C09@49.5, DM_C09@50.0, DF_C09@50.0 |

**TABLE 5 |** Optimal MQM models for traits evaluated in BolTBDH using 1,881 markers within $Y_{12}$ dataset. Epistatic interactions [$QTL_1 \times QTL_2$] calculated using penalties assigned from 1,000 permutations of scantwo() and included when $p_{fv1} < 0.05$.

| | Model |
|---|---|
| *Architecture* | |
| **LT** | ~ 3@5.9 + 4@15.0 + 9@9.0 + [4@15.0 × 9@9.0] + [5@39.5 × 6@28.3] |
| **MH** | NA |
| *Biomass* | |
| **MS** | ~ 5@39.5 + [3@0 × 5@40.3] |
| **VG** | ~ 4@2.4 + 5@39.9 + 7@43.4 + [4@0.5 × 4@20.5] |
| *Leaf morphology* | |
| **LA** | ~ 1@3.4 + 3@0.7 + 6@18.7 + 7@37.0 + [3@0 × 9@48.5] + [3@0 × 7@36.6] + [7@36.9 × 9@24.4] + [1@2.6 × 9@49.5] + [6@18.7 × 7@36.7] + [1@2.6 × 3@0.0] + [2@3.1 × 2@28.5] |
| **LM** | ~ 3@0.7 + 3@53.5 + 7@39.5 + [3@0.7 × 3@53.5] + [2@5.5 × 3@0.7] |
| **LC** | ~ 9@15.1 + [5@3.8 × 9@15.1] |
| *Bud morphology* | |
| **FC** | ~ 3@55.7 |
| **SE** | ~ 8@38.0 + [5@7.7 × 5@21.3] |
| **SF** | ~ 4@50.3 + [2@40.2 × 4@50.5] |
| **SH** | ~ 1@2.1 + [1@0.2 × 1@20.2] |
| **SS** | ~ 1@6.1 |
| **ST** | ~ 1@3.2 + [5@7.5 × 5@22.9] |
| **BS** | ~ 1@1.3 + 3@36.8 +5@43.0 + 6@3.8 + [1@1.3 × 5@39.5] +[5@43 × 6@3.9] |
| **BU** | ~ 3@1.7 + 4@51.5 |
| *Head morphology* | |
| **BR** | ~ 8@23.2 + 9@49.5 + [8@21.4 × 9@49.5] |
| **HC** | ~ 6@23.0 + 9@48.8 + [3@53.6 × 9@49.5] + [5@1.4 × 9@49.5] + [3@53.6 × 8@22.8] |
| **HD** | ~ 5@2.9 + 7@43.6/46.5 + [5@2.9 × 7@44.1] + [1@1.1 × 5@1.5] |
| **HE** | ~ 6@38.5 + 8@28.8 + 9@47.7 + [6@38.5 × 9@47.7] + [2@5.5 × 9@47.7] |
| **HS** | ~ 2@41.7 + 8@20.6 + 9@37.1 + [2@41.7 × 9@37.1] + [8@20.9 × 9@48.8] + [4@51.8 × 9@39] |
| **HU** | ~ 4@34.2 + 9@5.6 + 9@48.8 + [4@34.2 × 9@49.5] |
| **OQ** | ~ 3@57.0 + 4@33.3 + 8@24.0 + 9@49.5 + [8@25.5 × 9@49.5] + [5@1.3 × 9@49.5] + [3@53.6 × 8@23.3] |
| *Phenology* | |
| **DM** | ~ 3@6.4 + 9@50.0 + [3@6.4 × 9@50.0] + [3@6.4 × 7@42.0] |
| **DF** | ~ 3@6.4 + 9@50.0 + [3@6.4 × 9@50.0] |
| **HA** | ~ 5@4.0 + 6@25.9 + 7@41.2 + [9@9.5 × 9@10.7] + [5@36.6 × 5@37.3] |

× 1@20.2]) co-localized with the bud morphology hotspot $Bud_1$. $Bud_1$ QTL include the homologous candidates *AP2* (Bo1g004960), in agreement with Zhang et al. (2018). Further evaluation of *AP2* (Bo1g004960) homologs and other floral developmental candidates (**Table 6**) in the $Bud_1$ hotspot may prove useful for improvement of bud morphology traits.

Small flower buds are preferred in broccoli, but heat-tolerant germplasm typically exhibits larger flower buds. MQM modeling of bead size in BolTHDH resulted in a complex model trait model: BS ~ $Bud_1$ + 3@36.8 + $Bio_5$ + 6@3.8 + [$Bud_1 \times Bio_5$] + [$Bio_5 \times 6@3.9$], suggesting complex genetic control of this trait.

Unequal-sized flower buds are a common horticultural defect in broccoli and bud uniformity requires an arrest of enlargement of older buds until younger buds reach an equivalent size, requiring complex coordination (Roeder et al., 2010). Lin et al. (2018) identified a QTL within CO6 (*qCQ-6*) associated with a reduction in uneven-sized flower buds and identified *PAN* and the most probable candidate within this interval, exhibiting strongly differential expression in floral bud at harvest stage. In the BolTBDH model of flower bud uniformity (BU ~ $Lea_3$ + 4@51.5), the *PAN* homolog Bo6g107140 was not harbored within the identified BU QTL.

## Head Quality

For heading quality traits, the hotspot $HQ_9$ was remarkably pronounced within MQM analysis of BolTBDH. $HQ_9$ is syntenic with the telomeric region of the short arm of *Arabidopsis* Chr5 (O'neill and Bancroft, 2000), and this region has previously been shown to carry the homologs of the key flowering-time and vernalization-response genes *TLF2*, *COL1*, *CO*, and *FLC* (Osborn et al., 1997; Lagercrantz et al., 2002; Lin et al., 2005; Okazaki et al., 2007; Uptmoor et al., 2008; Iniguez-Luy et al., 2009; Hasan et al., 2016; Shea et al., 2018). Razi et al. (2008) mapped *BoFLC1* to the end of C09, and homology searches in the BOLv.2 genome indicated that two *FLC* copies (Bo9g173370 and Bo9g173400) appear to be harbored within the $HQ_9$ hotspot. These putative *BoFLC1* copies are located ~22 Kbp apart and may have been considered as a single copy in previous studies. In broccoli and cauliflower, this region has been implicated in vernalization requirement response (Bohuon et al., 1998; Rae et al., 1999), heat-tolerance (Branham et al., 2017), temperature dependent curd induction (Hasan et al., 2016), variation in heading response to temperature (Lin et al., 2019) and as a target for domestication due to a sharp increase in linkage disequilibrium when comparing improved broccoli and landrace broccoli genotypes (Stansell et al., 2018). Here, we identified $HQ_9$ as containing disproportionately many key heading-quality broccoli QTL: BU_C04@51.5, BR_C09@49.5, HC_C09@48.8, HU_C09@48.8, HE_C09@47.7, and OQ_C09@49.5, as well as two phenology QTL, DM_C09@50.0 and DF_C09@50.0.

Broccoli is characterized by strong suppression of bract elongation in the inflorescence and the "leaf in curd" bracting phenotype has been previously linked to high temperature stress (>22°C) (Booij and Struik, 1990). Kop et al. (2003) identified a role *Boap1-a* in bracting suppression within broccoli and cauliflower heads, although the authors suggested that additional candidates may be involved in bract development, e.g., *BoFUL*. Neither *AP1* (Bo2g062650, Bo6g095760, Bo6g095760, Bo6g108600), or *FUL* (Bo2g161210, Bo7g098190, Bo9g014400) homologs cosegregated with bracting loci identified within the BolTBDH MQM bracting model.

Compact broccoli heads are less susceptible to damage and are more efficient to ship. In broccoli, the degree of head compactness is a consequence of a short rachis at a large angle. In a $F_2$ *B. oleracea* cross, Lan and Paterson (2000) identified a C04 QTL (EW4D04w+7) likely implicated in curd density. A more complex head compactness model was observed in BolTBDH (HC ~ HC_6@23.0 + $HQ_9$ + [$HQ_9 \times 3@53.6$] + [$HQ_9 \times 5@1.4$] + [$HQ_8 \times 3@53.6$]).

**TABLE 6 |** For traits (Trait) evaluated within BolTBDH, the MQM QTL (**QTL**) determined by 95% Bayesian confidence intervals or ± 1 Mbp from LOD peak is (**Candidate**) intersected with homologous candidates (**Homolog**) identified by literature review/TAIR/EnsemblePlants.

| Trait | QTL | Homolog | Candidate | Reference |
|---|---|---|---|---|
| **LT** | LT_C03@5.9 | *VIN3* | Bo3g019340 | (Lin et al., 2005; Matschegewski et al., 2015; Ridge et al., 2015; Shea et al., 2018) |
| | LT_C04@15 | *TSF* | Bo4g061100 | (Shen et al., 2018) |
| | LT_C09@9.0 | *GRF6* | Bo9g018730 | (Wang et al., 2010; Leijten et al., 2018) |
| | | *FD* | Bo9g024710 | (Siriwardana and Lamb, 2012; Matschegewski et al., 2015; Leijten et al., 2018) |
| **MA** | MS_C05@39.5 | *BRC1* | Bo1g117490 | (Muntha et al., 2018; Shah et al., 2018; Lu et al., 2019) |
| **VG** | VG_C04@2.4 | *SPL9* | Bo4g015800 | (Siriwardana and Lamb, 2012; Leijten et al., 2018) |
| | | *FPA* | Bo4g019780 | (Lin et al., 2005; Leijten et al., 2018; Shea et al., 2018) |
| | | *ARL* | Bo4g021250 | (Wang et al., 2010) |
| | | *SOC1* | Bo4g024850 | (Lin et al., 2005; Siriwardana and Lamb, 2012; Matschegewski et al., 2015; Ridge et al., 2015; Leijten et al., 2018; Lin et al., 2018) |
| | | *ELF4* | Bo(4g025620/4g025580) | (Leijten et al., 2018) |
| | VG_C05@39.9 | *REM1* | Bo(5g136900/5g136880) | (Duclos and Björkman, 2008) |
| | | *BRC1* | Bo5g117410 | (Muntha et al., 2018; Shah et al., 2018; Lu et al., 2019) |
| | VG_C07@43.4 | *REM1* | Bo(7g115340/7g115310) | (Duclos and Björkman, 2008) |
| | | *VIN3* | Bo7g114310 | (Lin et al., 2005; Matschegewski et al., 2015; Ridge et al., 2015; Shea et al., 2018) |
| **LA** | LA_C03@0.7 | *LMI1* | Bo3g002560 | (Siriwardana and Lamb, 2012; Ni et al., 2017) |
| | LA_C06@18.7 | *GCT* | Bo6g051250 | (Gillmor et al., 2014) |
| | LA_C07@36.6 | *GIF1* | Bo7g093130 | (Wang et al., 2010; Siriwardana and Lamb, 2012) |
| **LM** | LM_C03@0.7 | *LMI1* | Bo3g002560 | (Siriwardana and Lamb, 2012; Ni et al., 2017) |
| **LC** | LC_C09@15.1 | *MAH1* | Bo9g053360 | |
| | | | Bo9g053340 | (Lee et al., 2015b) |
| | | | Bo9g053260 | |
| | | | Bo9g053220 | |
| | | | Bo9g053170 | |
| **FC** | FC_C03@55.7 | *CCD4* | Bo3g158650 | (Zhang et al., 2015) |
| **SE** | SE_C08@36.8 | *RAV1* | Bo8g107500 | (Siriwardana and Lamb, 2012) |
| **SH** | SH_C01@2.1 | *AP2* | Bo1g004960 | (Siriwardana and Lamb, 2012; Matschegewski et al., 2015; Branham et al., 2017; Zhang et al., 2018) |
| | | *AG* | Bo1g020110 | (Siriwardana and Lamb, 2012; Lin et al., 2019) |
| **SS** | SS_C01@6.1 | *AP2* | Bo1g004960 | (Siriwardana and Lamb, 2012; Matschegewski et al., 2015; Branham et al., 2017; Zhang et al., 2018) |
| | | *AG* | Bo1g020110 | (Siriwardana and Lamb, 2012; Lin et al., 2019) |
| **ST** | ST_C01@3.2 | *AP2* | Bo1g004960 | (Siriwardana and Lamb, 2012; Matschegewski et al., 2015; Branham et al., 2017; Zhang et al., 2018) |
| | | AG | Bo1g020110 | (Siriwardana and Lamb, 2012; Lin et al., 2019) |
| **BS** | BS_C01@1.3 | *AP2* | Bo1g004960 | (Siriwardana and Lamb, 2012; Matschegewski et al., 2015; Branham et al., 2017; Zhang et al., 2018) |
| | | *FD* | Bo1g006110 | (Siriwardana and Lamb, 2012; Matschegewski et al., 2015; Leijten et al., 2018) |
| | | *ROT3* | Bo1g005700 | (Wang et al., 2010) |
| | BS_C03@36.8 | *LFY* | Bo3g109270 | (Duclos and Björkman, 2008; Siriwardana and Lamb, 2012; Leijten et al., 2018; Sun et al., 2018; Lin et al., 2019) |
| | | *FAS2* | Bo3g101080 | (Boseon et al., 2019) |
| | | *GRF6* | Bo3g099210 | (Wang et al., 2010; Leijten et al., 2018) |
| | BS_C05@43.0 | *REM1* | Bo(5g136900/5g136880) | (Duclos and Björkman, 2008) |
| | BS C07@9.9 | *REM1* | Bo(7g054150/7g054160) | (Duclos and Björkman, 2008) |
| **BU** | BU_C03@1.7 | *LMI1* | Bo3g002560 | (Siriwardana and Lamb, 2012; Ni et al., 2017) |
| | | *FY* | Bo3g009200 | (Lin et al., 2005; Okazaki et al., 2007; Siriwardana and Lamb, 2012; Lin et al., 2019) |
| | | *REM1* | Bo3g007530 | (Duclos and Björkman, 2008) |
| | | *EMF1* | Bo3g007090 | (Okazaki et al., 2007;Siriwardana and Lamb, 2012) |
| | | *FLC* | Bo3g005470 | (Okazaki et al., 2007; Matschegewski et al., 2015; Ridge et al., 2015; Hasan et al., 2016; Lin et al., 2018; Lin et al., 2019) |
| **BR** | *BR*_C08@23.2 | CDF5 | Bo8g076530 | (Shen et al., 2018) |
| | | *REM1* | Bo8g071450 | (Duclos and Björkman, 2008) |
| | *BR*_C09@49.5 | FLC | Bo(9g173400/9g173370) | (Okazaki et al., 2007; Matschegewski et al., 2015; Ridge et al., 2015; Hasan et al., 2016; Irwin et al., 2016; Lin et al., 2018; Lin et al., 2019) |
| | | *GRF8* | Bo9g172070 | (Wang et al., 2010) |
| | | *CO* | Bo9g163730 | (Osborn et al., 1997; Bohuon et al., 1998; Rae et al., 1999; Axelsson et al., 2001; Okazaki et al., 2007; Irwin et al., 2016; Leijten et al., 2018) |
| | | *COL1* | Bo9g163720 | (Lagercrantz et al., 2002) |
| **HC** | HC C06@23.0 | *ARL* | Bo6g076730 | (Wang et al., 2010) |
| | | *LMI2* | Bo6g077600 | (Siriwardana and Lamb, 2012) |
| | HC_C09@48.8 | *SEP1* | Bo9g163790 | (Varaud et al., 2011; Siriwardana and Lamb, 2012; Zhang et al., 2018) |

(*Continued*)

**TABLE 6 |** Continued

| Trait | QTL | Homolog | Candidate | Reference |
|---|---|---|---|---|
| | | *CO* | Bo9g163730 | (Osborn et al., 1997; Bohuon et al., 1998; Rae et al., 1999; Axelsson et al., 2001; Okazaki et al., 2007; Irwin et al., 2016; Leijten et al., 2018) |
| | | *COL1* | Bo9g163720 | (Lagercrantz et al., 2002) |
| | | *FLC* | Bo(9g173400/9g173370) | (Okazaki et al., 2007; Matschegewski et al., 2015; Ridge et al., 2015; Hasan et al., 2016; Irwin et al., 2016; Lin et al., 2018; Lin et al., 2019) |
| | | *GRF8* | Bo9g172070 | (Wang et al., 2010) |
| **HD** | HD_C05@2.9 | *BIGPETAL* | Bo5g010880 | (Wang et al., 2010; Varaud et al., 2011) |
| | HD_ C07@43.6/46.5 | *REM1* | Bo(7g115340/7g115310) | (Duclos and Björkman, 2008) |
| | | *FD* | Bo7g117660 | (Siriwardana and Lamb, 2012; Matschegewski et al., 2015; Leijten et al., 2018) |
| | | *AP2* | Bo7g118400 | (Siriwardana and Lamb, 2012; Matschegewski et al., 2015; Branham et al., 2017; Zhang et al., 2018) |
| | | *ROT3* | Bo7g117920 | (Wang et al., 2010) |
| **HE** | HE_C06@38.5 | *TSF* | Bo6g120900 | (Shen et al., 2018) |
| | HE_C08@28. | *AP3* | Bo9g161800 | (Varaud et al., 2011; Siriwardana and Lamb, 2012; Zhang et al., 2018) |
| | HE C09@47.7 | *CO* | Bo9g163730 | (Osborn et al., 1997; Bohuon et al., 1998; Rae et al., 1999; Axelsson et al., 2001; Okazaki et al., 2007; Irwin et al., 2016; Leijten et al., 2018) |
| | | *COL1* | Bo9g163720 | (Lagercrantz et al., 2002) |
| | | *SEP1* | Bo9g163790 | (Varaud et al., 2011; Siriwardana and Lamb, 2012; Zhang et al., 2018) |
| | | *TFL2* | Bo9g159960 | (Okazaki et al., 2007; Duclos and Björkman, 2008; Siriwardana and Lamb, 2012; Schiessl et al., 2015; Branham et al., 2017; Leijten et al., 2018) |
| **HS** | *HS* C02@41.7 | UFO | Bo(2g121010/2g121010) | (Duclos and Björkman, 2008; Siriwardana and Lamb, 2012) |
| | *HS* C08@20.6 | REM1 | Bo8g071450 | (Duclos and Björkman, 2008) |
| | | *ARF5* | Bo8g069820 | (Siriwardana and Lamb, 2012; Zheng et al., 2019) |
| **HU** | HU_C04@34.2 | *AP3* | Bo4g120010 | (Varaud et al., 2011; Siriwardana and Lamb, 2012; Zhang et al., 2018) |
| | | *REM1* | Bo4g140670 | (Duclos and Björkman, 2008) |
| | | *SPL15* | Bo4g109710 | (Siriwardana and Lamb, 2012; Leijten et al., 2018) |
| | HU_C09@5.6 | *FPF1* | Bo9g011550 | (Schiessl et al., 2015) |
| | | *CO* | Bo9g011530 | (Osborn et al., 1997; Bohuon et al., 1998; Rae et al., 1999; Axelsson et al., 2001; Okazaki et al., 2007; Irwin et al., 2016; Leijten et al., 2018) |
| | | *GIF1* | Bo9g010000 | (Wang et al., 2010; Siriwardana and Lamb, 2012) |
| | HU_C09@48.8 | CO | Bo9g163730 | (Osborn et al., 1997; Bohuon et al., 1998; Rae et al., 1999; Axelsson et al., 2001; Okazaki et al., 2007; Irwin et al., 2016; Leijten et al., 2018) |
| | | *COL1* | Bo9g163720 | (Lagercrantz et al., 2002) |
| | | *TFL2* | Bo9g159960 | (Okazaki et al., 2007; Duclos and Björkman, 2008; Siriwardana and Lamb, 2012; Schiessl et al., 2015; Branham et al., 2017; Leijten et al., 2018) |
| **OQ** | OQ_C03@57 | *AG* | Bo3g157480 | (Siriwardana and Lamb, 2012; Lin et al., 2019) |
| | | FD | Bo3g156810 | (Siriwardana and Lamb, 2012; Matschegewski et al., 2015; Leijten et al., 2018) |
| | OQ_C04@33.3 | *AP3* | Bo4g120010 | (Varaud et al., 2011; Siriwardana and Lamb, 2012; Zhang et al., 2018) |
| | OQ_C08@24 | *CDF5* | Bo8g076530 | (Shen et al., 2018) |
| | | *REM1* | Bo8g071450 | (Duclos and Björkman, 2008) |
| | OQ_C09@49.7 | *FLC* | Bo(9g173400/9g173370) | (Okazaki et al., 2007; Matschegewski et al., 2015; Ridge et al., 2015; Hasan et al., 2016; Irwin et al., 2016; Lin et al., 2018; Lin et al., 2019) |
| | | *GRF8* | Bo9g172070 | (Wang et al., 2010) |
| | | *CO* | Bo9g163730 | (Osborn et al., 1997; Bohuon et al., 1998; Rae et al., 1999; Axelsson et al., 2001; Okazaki et al., 2007; Irwin et al., 2016; Leijten et al., 2018) |
| | | *COL1* | Bo9g163720 | (Lagercrantz et al., 2002) |
| **DM** | DM C03@6.4 | *FLC* | Bo3g024250 | (Okazaki et al., 2007; Matschegewski et al., 2015; Ridge et al., 2015; Hasan et al., 2016; Irwin et al., 2016; Lin et al., 2018; Lin et al., 2019) |
| | | *TFL* | Bo3g012730 | (Okazaki et al., 2007; Duclos and Björkman, 2008; Siriwardana and Lamb, 2012; Schiessl et al., 2015; Branham et al., 2017; Leijten et al., 2018) |
| | DM C09@50.0 | *FLC* | Bo(9g173400/9g173370) | (Okazaki et al., 2007; Matschegewski et al., 2015; Ridge et al., 2015; Hasan et al., 2016; Irwin et al., 2016; Lin et al., 2018; Lin et al., 2019) |
| | | *GRF8* | Bo9g172070 | (Wang et al., 2010) |
| | | *SEP1* | Bo9g163790 | (Varaud et al., 2011; Siriwardana and Lamb, 2012; Zhang et al., 2018) |
| | | *CO* | Bo9g163730 | (Osborn et al., 1997; Bohuon et al., 1998; Rae et al., 1999; Axelsson et al., 2001; Okazaki et al., 2007; Irwin et al., 2016; Leijten et al., 2018) |
| | | *COL1* | Bo9g163720 | (Lagercrantz et al., 2002) |
| **DF** | DF_C03@6.4 | *FLC* | Bo3g024250 | (Okazaki et al., 2007; Matschegewski et al., 2015; Ridge et al., 2015; Hasan et al., 2016; Irwin et al., 2016; Lin et al., 2018; Lin et al., 2019) |
| | | *VIN3* | Bo3g019340 | (Lin et al., 2005; Matschegewski et al., 2015; Ridge et al., 2015; Shea et al., 2018) |
| | DF_C09@50 | *FLC* | Bo(9g173400/9g173370) | (Okazaki et al., 2007; Matschegewski et al., 2015; Ridge et al., 2015; Hasan et al., 2016; Irwin et al., 2016; Lin et al., 2018; Lin et al., 2019) |

(*Continued*)

**TABLE 6** | Continued

| Trait | QTL | Homolog | Candidate | Reference |
|---|---|---|---|---|
| | | *GRF8* | Bo9g172070 | (Wang et al., 2010) |
| | | *SEP1* | Bo9g163790 | (Varaud et al., 2011; Siriwardana and Lamb, 2012; Zhang et al., 2018) |
| | | *CO* | Bo9g163730 | (Osborn et al., 1997; Bohuon et al., 1998; Rae et al., 1999; Axelsson et al., 2001; Okazaki et al., 2007; Irwin et al., 2016; Leijten et al., 2018) |
| | | *COL1* | Bo9g163720 | (Lagercrantz et al., 2002) |

Along with head compactness, head diameter at maturity is an important element of high yielding cultivars. In three *B. oleracea* $F_2$ populations, Lan and Paterson (2000) identified 14 curd width QTL on chromosomes C01, C03, C4, C5, C7, C8, and C9. Within a broccoli × broccoli mapping population, Walley et al. (2012) identified QTL for head diameter on linkage groups C2, C4, C6, C7, and C9. Head diameter within BolTBDH was captured by the MQM model HD ~ HD_C05 @2.9 + HD_C07@43.6/46.5 + [HD_C05@2.9 × HD_C07@43.6/46.5] + [$Bud_1$ × HD_C05@2.9].

Head extension above lead rosette is a useful trait in broccoli by reducing labor during harvest. Alternatively, late stem elongation may be a useful to protect the head during growth. The MQM model of head extension is complex: HE ~ $HQ_9$ + $HQ_8$ + C06@38.5 + [$HQ_9$ × 6@38.5] + [$HQ_9$ × 2@5.5].

Convex head shape is an important trait in broccoli by allowing the crown to shed water, thereby reducing disease incidence and exhibits complex control HC ~ $HQ_8$ + C02@41.7 + C09@37.1 + [$HQ_8$ x $HQ_9$] + [2@41.7 × 9@37.1].

As expected, overall broccoli heading quality is the most complex of the head quality traits, best captured by the MQM model: OQ ~ 3@57.0 + $HQ_4$ + $HQ_8$ + $HQ_9$ + [$HQ_8$ × 3@53.6] + [$HQ_8$ × $HQ_9$] + [$HQ_9$ × 5@1.3]. A simple control model of the broccoli heading-phenotype due to quantitative control of heading quality traits may be excluded given the MQM model determined in BolTBDH. Additionally, a constrictive-conditional model explaining the broccoli heading-phenotype seems less probable given the relative independence of heading quality traits. For example, the MQM models for HS and HU share $HQ_9$, but HS does not share $HQ_4$ with the overall heading quality model, nor does HU share $HQ_8$ with the overall heading quality model (**Figure S4**). The arrested-meristem broccoli heading-phenotype is best explained by a pleiotropic model — where a small number of genes within $HQ_9$ are implicated in multiple heading quality traits, and these $HQ_9$ genes exhibit important epistatic interactions with other heading quality loci.

### Phenology

In a previous study of days to flowering within a different *albogabra* × *italica* mapping population, Bohuon et al. (1998) identified QTL on C02, C03, C05, and C09. In a QTL-seq analysis of broccoli × cabbage, Shu et al. (2018) identified three flowering time regions: C02@0.9–2.9 Mb, C03@1.8–20 Mb, and C06@5.0–5.6 Mb. Only the C03@1.8–20 Mb region collocated with the DF QTL identified in BolTBDH (DF_C03@6.4). Using a relative expression approach, Abuyusuf et al. (2019) report sequence based variations in *BoFLC1.C9* (C09:51.0–51.0 Mb) implicated in early and late flowering cabbage genotypes, in agreement with the DM_C09@50.0 and DF_C09@50.0 QTL identified in BolTBDH. In a study of curd initiation in DH cauliflower, Hasan et al. (2016) identified a temperature-dependent time to curd induction QTL on C09 at 49.4 Mb, closely collocating with DM_C09@50.0 and DF_C09@50.0 and identified additional days to flowering QTL on C04, C05, C06, and C07. Within BolTBDH, days to head maturity and flowering appear to be each strongly influenced by two hotspots $HQ_9$ × $PHE_3$ given by the QTL pairs (DM C03_6.4 and DF_C03@6.4) and (DM_C09@49.7 and DF_C09@49.7) and these pairs exhibit strong epistatic effects ([DM_3@6.4 × DM_9@50.0]; $p_{fv1}$ << 0.01) and [DM_C09@50.0 × DF_C09@50.0] (pfv1 << 0.01). One additional DM epistatic effect was detected ([HQ9 x 7@DM_42.0]; $p_{fv1}$ = 0.023). Interestingly, $HQ_9$ collocates with the region of strongest genome-wide segregation distortion ($P_1$ allele: $f$ = 0.76). If late-flowering DHs were underrepresented during tissue culture or seed regeneration, the $P_1$ allele and surrounding region would exhibit segregation enrichment.

Lan and Paterson (2000) identified 15 "days from budding to flowering" QTL, analogous to the holding ability trait measured in BolTHDH population. In BolTBDH, "days from head maturity trait to flowering" was best explained by a complex MQM model: HA ~ 5@4.0 + 6@25.9 + 7@41.2 + [9@9.5 × 9@10.7] + [5@36.6 × 5@37.3] and no likely homologous candidates were identified.

## Conclusions

Evaluation of the BolTBDH population provides new insights into key genomic regions and developmental candidates that define heading broccoli by identifying essential QTL implicated in these phenotypic outcomes. These results support a pleiotropic model of a heading broccoli phenotype. This work demonstrates several key genomic hotspots as essential for the phenotypes observed within this study, and these QTL and markers may prove useful for future marker-assisted breeding efforts. The phenomic and genomic dataset provided herein may be used for additional mapping studies and be integrated with previous work (e.g. metabolic and pathogen resistance studies).

## DATA AVAILABILITY

The datasets used for this study are included in *Stansell_2019_Supp_Data.zip*. The code used for this study is available at:

- https://github.com/zacharystansell/BolTBDH
- https://github.com/zacharystansell/ratervar

## AUTHOR CONTRIBUTIONS

ZS and TB conducted experimental design, ZS conducted phenotyping and statistical analyses. MF provided experimental germplasm. All authors wrote the manuscript.

## FUNDING

This work is supported by Specialty Crop Research Initiative grant no. 2016-51181-25402 from the USDA National Institute of Food and Agriculture.

## ACKNOWLEDGMENTS

We thank Miranda Penney and Aleah Butler-Jones for assistance with field phenotyping. Roberto Lazano, Deniz Akdemir, Jian Hua, Jacob Landis, and Sandra Branham provided many helpful comments and suggestions. The UWBC DNA Sequencing Facility provided valuable sequencing services.

## SUPPLEMENTARY MATERIAL

The Supplementary Material for this article can be found online at: https://www.frontiersin.org/articles/10.3389/fpls.2019.01104/full#supplementary-material

## REFERENCES

Abuyusuf, M., Nath, U. K., Kim, H.-T., Islam, M. R., Park, J.-I., and Nou, I.-S. (2019). Molecular markers based on sequence variation in BoFLC1.C9 for characterizing early-and late-flowering cabbage genotypes. *BMC Genet.* 20, 42. doi: 10.1186/s12863-019-0740-1

Arends, D., Prins, P., Jansen, R. C., and Broman, K. W. (2010). R/qtl: high-throughput multiple QTL mapping. *Bioinformatics* 26, 2990–2992. doi: 10.1093/bioinformatics/btq565

Atallah, S. S., Gómez, M. I., and Björkman, T. (2014). Localization effects for a fresh vegetable product supply chain: broccoli in the eastern united states. *Food Policy* 49, 151–159. doi: 10.1016/j.foodpol.2014.07.005

Axelsson, T., Shavorskaya, O., and Lagercrantz, U. (2001). Multiple flowering time QTLs within several brassica species could be the result of duplicated copies of one ancestral gene. *Genome* 44, 856–864. doi: 10.1139/g01-082

Berardini, T. Z., Reiser, L., Li, D., Mezheritsky, Y., Muller, R., Strait, E., et al. (2015). The *Arabidopsis* information resource: making and mining the "gold standard" annotated reference plant genome. *Genesis* 53, 474–485. doi: 10.1002/dvg.22877

Björkman, T., and Pearson, K. J. (1998). High temperature arrest of inflorescence development in broccoli (*Brassica oleracea* var. *Italica* l.). *J. Exp. Bot.* 49, 101–106. doi: 10.1093/jxb/49.318.101

Bohuon, E. J. R., Ramsay, L. D., Craft, J. A., Arthur, A. E., Marshall, D. F., Lydiate, D. J., et al. (1998). The association of flowering time quantitative trait loci with duplicated regions and candidate loci in *Brassica oleracea. Genetics* 150, 393–401.

Booij, R., and Struik, P. (1990). Effects of temperature on leaf and curd initiation in relation to juvenility of cauliflower. *Sci. Hortic.* 44, 201–214. doi: 10.1016/0304-4238(90)90120-4

Boseon, B., Bilichak, A., and Kovalchuk, I. (2019). Transgenerational response to heat stress in the form of differential expression of noncoding RNA fragments in *Brassica rapa* plants. *Plant Genome* 12, 180022 doi: 10.3835/plantgenome2018.04.0022

Branham, S. E., and Farnham, M. W. (2017). Genotyping-by-sequencing of waxy and glossy near-isogenic broccoli lines. *Euphytica* 213, 84. doi: 10.1007/s10681-017-1873-9

Branham, S. E., Stansell, Z. J., Couillard, D. M., and Farnham, M. W. (2017). Quantitative trait loci mapping of heat tolerance in broccoli (*Brassica oleracea* var. *Italica*) using genotyping-by-sequencing. *Theor. Appl. Genet.* 130, 529–538. doi: 10.1007/s00122-016-2832-x

Broman, K. W., Wu, H., Sen, Ś., and Churchill, G. A. (2003). R/qtl: QTL mapping in experimental crosses. *Bioinformatics* 19, 889–890. doi: 10.1093/bioinformatics/btg112

Brown, A. F., Yousef, G. G., Chebrolu, K. K., Byrd, R. W., Everhart, K. W., Thomas, A., et al. (2014). High-density single nucleotide polymorphism (SNP) array mapping in *Brassica oleracea*: identification of qtl associated with carotenoid variation in broccoli florets. *Theor. Appl. Genet.* 127, 2051–2064. doi: 10.1007/s00122-014-2360-5

Camargo, L. E. A., and Osborn, T. C. (1996). Mapping loci controlling flowering time in *Brassica oleracea. Theor. Appl. Genet.* 92, 610–616. doi: 10.1007/BF00224565

Cheng, F., Sun, R., Hou, X., Zheng, H., Zhang, F., Zhang, Y., et al. (2016). Subgenome parallel selection is associated with morphotype diversification and convergent crop domestication in *Brassica rapa* and *Brassica oleracea. Nat. Genet.* 48, 1218. doi: 10.1038/ng.3634

Duclos, D. V., and Björkman, T. (2008). Meristem identity gene expression during curd proliferation and flower initiation in *Brassica oleracea. J. Exp. Bot.* 59, 421–433. doi: 10.1093/jxb/erm327

Elshire, R. J., Glaubitz, J. C., Sun, Q., Poland, J. A., Kawamoto, K., Buckler, E. S., et al. (2011). A robust, simple genotyping-by-sequencing (GBS) approach for high diversity species. *PLoS One* 6, e19379. doi: 10.1371/journal.pone.0019379

Farnham, M. W. (1998). Doubled-haploid broccoli production using anther culture: effect of anther source and seed set characteristics of derived lines. *J. Am. Soc. Hortic. Sci.* 123, 73–77. doi: 10.21273/JASHS.123.1.73

Farnham, M. W., and Björkman, T. (2011). Evaluation of experimental broccoli hybrids developed for summer production in the eastern united states. *HortScience* 46, 858–863. doi: 10.21273/HORTSCI.46.6.858

Francisco, M., Ali, M., Ferreres, F., Moreno, D. A., Velasco, P., and Soengas, P. (2016). Organ-specific quantitative genetics and candidate genes of phenylpropanoid metabolism in *Brassica oleracea. Front. Plant Sci.* 6, 1240. doi: 10.3389/fpls.2015.01240

Gao, M., Li, G., McCombie, W. R., and Quiros, C. F. (2005). Comparative analysis of a transposon-rich *Brassica oleracea* bac clone with its corresponding sequence in *A. thaliana. Theor. Appl. Genet.* 111, 949–955. doi: 10.1007/s00122-005-0029-9

Gao, M., Li, G., Yang, B., Qiu, D., Farnham, M., and Quiros, C. (2007). High-density *Brassica oleracea* linkage map: identification of useful new linkages. *Theor. Appl. Genet.* 115, 277–287. doi: 10.1007/s00122-007-0568-3

Gillmor, C. S., Silva-Ortega, C. O., Willmann, M. R., Buendía-Monreal, M., and Poethig, R. S. (2014). The *Arabidopsis* mediator CDK8 module genes CCT (MED12) and GCT (MED13) are global regulators of developmental phase transitions. *Development* 141, 4580–4589. doi: 10.1242/dev.111229

Glaubitz, J. C., Casstevens, T. M., Lu, F., Harriman, J., Elshire, R. J., Sun, Q., et al. (2014). TASSEL-GBS: a high capacity genotyping by sequencing analysis pipeline. *PloS One* 9, e90346. doi: 10.1371/journal.pone.0090346

Golicz, A. A., Bayer, P. E., Barker, G. C., Edger, P. P., Kim, H., Martinez, P. A., et al. (2016). The pangenome of an agronomically important crop plant *Brassica oleracea. Nat. Commun.* 7, 13390. doi: 10.1038/ncomms13390

Greer, S., Wen, M., Bird, D., Wu, X., Samuels, L., Kunst, L., et al. (2007). The cytochrome p450 enzyme CYP96a15 is the midchain alkane hydroxylase responsible for formation of secondary alcohols and ketones in stem cuticular wax of *Arabidopsis. Plant Physiol.* 145, 653–667. doi: 10.1104/pp.107.107300

Gromping, U. (2006). Relative importance for linear regression in R: the package relaimpo. *J. Stat. Software* 17(1), 1–27. doi: 10.18637/jss.v017.i01

Han, F., Cui, H., Zhang, B., Liu, X., Yang, L., Zhuang, M., et al. (2019). Map-based cloning and characterization of BoCCD4, a gene responsible for white/yellow petal color in *B. oleracea*. *BMC Genomics* 20, 242. doi: 10.1186/s12864-019-5596-2

Hasan, Y., Briggs, W., Matschegewski, C., Ordon, F., Stützel, H., Zetzsche, H., et al. (2016). Quantitative trait loci controlling leaf appearance and curd initiation of cauliflower in relation to temperature. *TAG. Theor. Appl. Genet.* 129, 1273–1288. doi: 10.1007/s00122-016-2702-6

Hatzig, S. V., Frisch, M., Breuer, F., Nesi, N., Ducournau, S., Wagner, M.-H., et al. (2015). Genome-wide association mapping unravels the genetic control of seed germination and vigor in *Brassica napus*. *Front. Plant Sci.* 6, 221. doi: 10.3389/fpls.2015.00221

He, Y., Wu, D., Wei, D., Fu, Y., Cui, Y., Dong, H., et al. (2017). Gwas, qtl mapping and gene expression analyses in *Brassica napus* reveal genetic control of branching morphogenesis. *Sci. Rep.* 7, 15971. doi: 10.1038/s41598-017-15976-4

Hu, J., Sadowski, J., Osborn, T. C., Landry, B. S., and Quiros, C. F. (1998). Linkage group alignment from four independent *Brassica oleracea* RFLP maps. *Genome* 41, 226–235. doi: 10.1139/g98-007

Iglesias-Bernabé, L., Madloo, P., Rodríguez, V. M., Francisco, M., and Soengas, P. (2019). Dissecting quantitative resistance to *Xanthomonas campestris* pv. *campestris* in leaves of *Brassica oleracea* by QTL analysis. *Sci. Rep.* 9, 2015. doi: 10.1038/s41598-019-38527-5

Iniguez-Luy, F. L., Lukens, L., Farnham, M. W., Amasino, R. M., and Osborn, T. C. (2009). Development of public immortal mapping populations, molecular markers and linkage maps for rapid cycling *Brassica rapa* and *Brassica oleracea*. *Theor. Appl. Genet.* 120, 31–43. doi: 10.1007/s00122-009-1157-4

Irwin, J. A., Soumpourou, E., Lister, C., Ligthart, J., Kennedy, S., and Dean, C. (2016). Nucleotide polymorphism affecting FLC expression underpins heading date variation in horticultural brassicas. *Plant J.* 87, 597–605. doi: 10.1111/tpj.13221

Kianian, S. F., and Quiros, C. F. (1992). Generation of a brassica oleracea composite RFLP map: linkage arrangements among various populations and evolutionary implications. *Theor. Appl. Genet.* 84, 544–554. doi: 10.1007/BF00224150

Kop, E. P., Teakle, G. R., McClenaghan, E. R., Lynn, J. R., and King, G. J. (2003). Genetic analysis of the bracting trait in cauliflower and broccoli. *Plant Sci.* 164, 803–808. doi: 10.1016/S0168-9452(03)00068-2

Lagercrantz, U., Kruskopf Osterberg, M., and Lascoux, M. (2002). Sequence variation and haplotype structure at the putative flowering-time locus COL1 of *Brassica nigra*. *Mol. Biol. Evol.* 19, 1474–1482. doi: 10.1093/oxfordjournals.molbev.a004210

Lan, T., and Paterson, A. H. (2001). Comparative mapping of QTLs determining the plant size of *Brassica oleracea*. *Theor. Appl. Genet.* 103, 383–397. doi: 10.1007/s001220100615

Lan, T. H., and Paterson, A. H. (2000). Comparative mapping of quantitative trait loci sculpting the curd of *Brassica oleracea*. *Genetics* 155, 1927–1954. doi: 10.1007/s001220100615

Landry, B. S., Hubert, N., Crete, R., Chang, M. S., Lincoln, S. E., and Etoh, T. (1992). A genetic map for *Brassica oleracea* based on RFLP markers detected with expressed DNA sequences and mapping of resistance genes to race 2 of *Plasmodiophora brassicae* (woronin). *Genome* 35, 409–420. doi: 10.1139/g92-061

Lee, J., Izzah, N. K., Choi, B.-S., Joh, H. J., Lee, S.-C., Perumal, S., et al. (2015a). Genotyping-by-sequencing map permits identification of clubroot resistance QTLs and revision of the reference genome assembly in cabbage (*Brassica oleracea* l.). *DNA Res.* 23, 29–41. doi: 10.1093/dnares/dsv034

Lee, J., Yang, K., Lee, M., Kim, S., Kim, J., Lim, S., et al. (2015b). Differentiated cuticular wax content and expression patterns of cuticular wax biosynthetic genes in bloomed and bloomless broccoli (*Brassica oleracea* var. *Italica*). *Process Biochem.* 50, 456–462. doi: 10.1016/j.procbio.2014.12.012

Leijten, W., Koes, R., Roobeek, I., and Frugis, G. (2018). Translating flowering time from *Arabidopsis thaliana* to *Brassicaceae* and *Asteraceae* crop species. *Plants* 7, 111. doi: 10.3390/plants7040111

Li, F., Kitashiba, H., Inaba, K., and Nishio, T. (2009). A *Brassica rapa* linkage map of EST-based SNP markers for identification of candidate genes controlling flowering time and leaf morphological traits. *DNA Res.* 16, 311–323. doi: 10.1093/dnares/dsp020

Li, G., Gao, M., Yang, B., and Quiros, C. F. (2003). Gene for gene alignment between the *Brassica* and *Arabidopsis* genomes by direct transcriptome mapping. *Theor. Appl. Genet.* 107, 168–180. doi: 10.1007/s00122-003-1236-x

Li, G., Zhang, G., Zhang, Y., Liu, K., Li, T., and Chen, H. (2015). Identification of quantitative trait loci for bolting and flowering times in Chinese kale (*Brassica oleracea* var. *Alboglabra*) based on ssr and srap markers. *J. Hortic. Sci. Biotechnol.* 90, 728–737. doi: 10.1080/14620316.2015.11668739

Li, H. (2013). "Aligning sequence reads, clone sequences and assembly contigs with BWA-MEM" in *arXiv* (Cambridge, USA: Broad Institute of Harvard and MIT), 1–3.

Li, Z., Mei, Y., Liu, Y., Fang, Z., Yang, L., Zhuang, M., et al. (2019). The evolution of genetic diversity of broccoli cultivars in China since 1980. *Sci. Hortic.* 250, 69–80. doi: 10.1016/j.scienta.2019.02.034

Lin, C.-W., Fu, S.-F., Liu, Y.-J., Chen, C.-C., Chang, C.-H., Yang, Y.-W., et al. (2019). Analysis of ambient temperature-responsive transcriptome in shoot apical meristem of heat-tolerant and heat-sensitive broccoli inbred lines during floral head formation. *BMC Plant Biol.* 19, 3. doi: 10.1186/s12870-018-1613-x

Lin, K., Chang, L., Lai, C., and Lo, H. (2013). Aflp mapping of quantitative trait loci influencing seven head-related traits in broccoli (*Brassica oleracea* var. *Italica*). *J. Hortic. Sci. Biotechnol.* 88, 257–268. doi: 10.1080/14620316.2013.11512964

Lin, S.-I., Wang, J.-G., Poon, S.-Y., Wang, S.-S., and Chiou, T.-J. (2005). Differential regulation of FLOWERING LOCUS C expression by vernalization in cabbage and *Arabidopsis*. *Plant Physiol.* 137, 1037–1048. doi: 10.1104/pp.104.058974

Lin, Y.-R., Lee, J.-Y., Tseng, M.-C., Lee, C.-Y., Shen, C.-H., Wang, C.-S., et al. (2018). Subtropical adaptation of a temperate plant (*Brassica oleracea* var. *Italica*) utilizes non-vernalization-responsive QTLs. *Sci. Rep.* 8, 13609. doi: 10.1038/s41598-018-31987-1

Liu, S., Liu, Y., Yang, X., Tong, C., Edwards, D., Parkin, I. A. P., et al. (2014). The *Brassica oleracea* genome reveals the asymmetrical evolution of polyploid genomes. *Nat. Commun.* 5, 3930. doi: 10.1038/ncomms4930

Lu, K., Peng, L., Zhang, C., Lu, J., Yang, B., Xiao, Z., et al. (2017). Genome-wide association and transcriptome analyses reveal candidate genes underlying yield-determining traits in *Brassica napus*. *Front. Plant Sci.* 8, 206. doi: 10.3389/fpls.2017.00206

Lu, K., Wei, L., Li, X., Wang, Y., Wu, J., Liu, M., et al. (2019). Whole-genome resequencing reveals *Brassica napus* origin and genetic loci involved in its improvement. *Nat. Commun.* 10, 1154. doi: 10.1038/s41467-019-09134-9

Matschegewski, C., Zetzsche, H., Hasan, Y., Leibeguth, L., Briggs, W., Ordon, F., et al. (2015). Genetic variation of temperature-regulated curd induction in cauliflower: elucidation of floral transition by genome-wide association mapping and gene expression analysis. *Front. Plant Sci.* 6, 720. doi: 10.3389/fpls.2015.00720

Muntha, S. T., Zhang, L., Zhou, Y., Zhao, X., Hu, Z., Yang, J., et al. (2018). Phytochrome A signal transduction 1 and CONSTANS-LIKE 13 coordinately orchestrate shoot branching and flowering in leafy *Brassica juncea*. *Plant Biotechnol. J.* 17, 1333–1343. doi: 10.1111/pbi.13057

Ni, X., Liu, H., Huang, J., and Zhao, J. (2017). LMI1-like genes involved in leaf margin development of *Brassica napus*. *Genetica* 145, 269–274. doi: 10.1007/s10709-017-9963-0

Okazaki, K., Sakamoto, K., Kikuchi, R., Saito, A., Togashi, E., Kuginuki, Y., et al. (2007). Mapping and characterization of FLC homologs and QTL analysis of flowering time in *Brassica oleracea*. *Theor. Appl. Genet.* 114, 595–608. doi: 10.1007/s00122-006-0460-6

O'neill, C. M., and Bancroft, I. (2000). Comparative physical mapping of segments of the genome of *Brassica oleracea* var. *Alboglabra* that are homoeologous to sequenced regions of chromosomes 4 and 5 of *Arabidopsis thaliana*. *Plant J.* 23, 233–243. doi: 10.1046/j.1365-313x.2000.00781.x

Osborn, T. C., Kole, C., Parkin, I. A., Sharpe, A. G., Kuiper, M., Lydiate, D. J., et al. (1997). Comparison of flowering time genes in *Brassica rapa*, *Brassica napus* and *Arabidopsis thaliana*. *Genetics* 146, 1123–1129.

Parkin, I. A., Koh, C., Tang, H., Robinson, S. J., Kagale, S., Clarke, W. E., et al. (2014). Transcriptome and methylome profiling reveals relics of genome dominance in the mesopolyploid *Brassica oleracea*. *Genome Biol.* 15, R77. doi: 10.1186/gb-2014-15-6-r77

Pink, D., Bailey, L., McClement, S., Hand, P., Mathas, E., Buchanan-Wollaston, V., et al. (2008). Double haploids, markers and QTL analysis in vegetable brassicas. *Euphytica* 164, 509–514. doi: 10.1007/s10681-008-9742-1

Potters, G., Pasternak, T. P., Guisez, Y., Palme, K. J., and Jansen, M. A. (2007). Stress-induced morphogenic responses: growing out of trouble? *Trends Plant Sci.* 12, 98–105. doi: 10.1016/j.tplants.2007.01.004

R-Core-Team. (2018). R: A language and environment for statistical computing. *FIX!*

R Core Team (2019). *R: A Language and Environment for Statistical Computing*. Vienna, Austria: R Foundation for Statistical Computing.

Rae, A. M., Howell, E. C., and Kearsey, M. J. (1999). More QTL for flowering time revealed by substitution lines in *Brassica oleracea*. *Heredity* 83, 586. doi: 10.1038/sj.hdy.6886050

Ramsay, L., Jennings, D., Kearsey, M. J., Marshall, D. F., Bohuon, E. J. R., Arthur, A. E., et al. (1996). The construction of a substitution library of recombinant backcross lines in *Brassica oleracea* for the precision mapping of quantitative trait loci. *Genome* 39, 558–567. doi: 10.1139/g96-071

Razi, H., Howell, E. C., Newbury, H. J., and Kearsey, M. J. (2008). Does sequence polymorphism of FLC paralogues underlie flowering time QTL in *Brassica oleracea*? *TAG. Theor. Appl. Genet.* 116, 179–192. doi: 10.1007/s00122-007-0657-3

Ren, J., Liu, Z., Du, J., Fu, W., Hou, A., and Feng, H. (2019). Fine-mapping of a gene for the lobed leaf, boll, in ornamental kale (*Brassica oleracea* L. var. *Acephala*). *Mol. Breed.* 39, 40. doi: 10.1007/s11032-019-0944-0

Ridge, S., Brown, P. H., Hecht, V., Driessen, R. G., and Weller, J. L. (2015). The role of BoFLC2 in cauliflower (*Brassica oleracea* var. *Botrytis* l.) reproductive development. *J. Exp. Bot.* 66, 125–135. doi: 10.1093/jxb/eru408

Roeder, A. H. K., Chickarmane, V., Cunha, A., Obara, B., Manjunath, B. S., and Meyerowitz, E. M. (2010). Variability in the control of cell division underlies sepal epidermal patterning in *Arabidopsis thaliana*. *PLoS Biol.* 8, e1000367. doi: 10.1371/journal.pbio.1000367

Ruffier, M., Kähäri, A., Komorowska, M., Keenan, S., Laird, M., Longden, I., et al. (2017). Ensembl core software resources: storage and programmatic access for DNA sequence and genome annotation. *Database (Oxford)* 2017, (1) bax020. doi: 10.1093/database/bax020

Schiessl, S., Iniguez-Luy, F., Qian, W., and Snowdon, R. J. (2015). Diverse regulatory factors associate with flowering time and yield responses in winter-type *Brassica napus*. *BMC Genomics* 16, 737. doi: 10.1186/s12864-015-1950-1

Sebastian, R. L., Howell, E. C., King, G. J., Marshall, D. F., and Kearsey, M. J. (2000). An integrated AFLP and RFLP *Brassica oleracea* linkage map from two morphologically distinct doubled-haploid mapping populations. *Theor. Appl. Genet.* 100, 75–81. doi: 10.1007/s001220050011

Sebastian, R. L., Kearsey, M. J., and King, G. J. (2002). Identification of quantitative trait loci controlling developmental characteristics of *Brassica oleracea* L. *Theor. Appl. Genet.* 104, 601–609. doi: 10.1007/s001220100743

Shah, S., Weinholdt, C., Jedrusik, N., Molina, C., Zou, J., Große, I., et al. (2018). Whole-transcriptome analysis reveals genetic factors underlying flowering time regulation in rapeseed (*Brassica napus* L.). *Plant Cell Environ.* 41, 1935–1947. doi: 10.1111/pce.13353

Shea, D. J., Itabashi, E., Takada, S., Fukai, E., Kakizaki, T., Fujimoto, R., et al. (2018). The role of FLOWERING LOCUS C in vernalization of *Brassica*: the importance of vernalization research in the face of climate change. *Crop Pasture Sci.* 69, 30–39. doi: 10.1071/CP16468

Shen, Y., Xiang, Y., Xu, E., Ge, X., and Li, Z. (2018). Major co-localized QTL for plant height, branch initiation height, stem diameter, and flowering time in an alien introgression derived *Brassica napus* DH population. *Front. Plant Sci.* 9, 390. doi: 10.3389/fpls.2018.00390

Shimano, S., Hibara, K.-I., Furuya, T., Arimura, S.-I., Tsukaya, H., and Itoh, J.-I. (2018). Conserved functional control, but distinct regulation, of cell proliferation in rice and *Arabidopsis* leaves revealed by comparative analysis of *GRF-INTERACTING FACTOR 1* orthologs. *Development* 145, dev159624. doi: 10.1242/dev.159624

Shu, J., Liu, Y., Zhang, L., Li, Z., Fang, Z., Yang, L., et al. (2018). Qtl-seq for rapid identification of candidate genes for flowering time in broccoli × cabbage. *Theor. Appl. Genet.* 131, 917–928. doi: 10.1007/s00122-017-3047-5

Siriwardana, N. S., and Lamb, R. S. (2012). The poetry of reproduction: the role of leafy in *Arabidopsis thaliana* flower formation. *Int. J. Dev. Biol.* 56, 207–221. doi: 10.1387/ijdb.113450ns

Sotelo, T., Cartea, M. E., Velasco, P., and Soengas, P. (2014). Identification of antioxidant capacity-related QTLs in *Brassica oleracea*. *PLoS One* 9(9), e107290. doi: 10.1371/journal.pone.0107290

Sotelo Pérez, T., Francisco Candeira, M., Cartea González, M. E., Rodríguez Graña, V. M., and Soengas Fernández, M. D. P. (2014). QTLs controlling antioxidant capacity in leaves and flower buds of *Brassica oleracea*. *PLoS One*. doi: 10.1371/journal.pone.0107290

Stansell, Z., Björkman, T., Branham, S., Couillard, D., and Farnham, M. W. (2017). Use of a quality trait index to increase the reliability of phenotypic evaluations in broccoli. *HortScience* 52, 1490–1495. doi: 10.21273/HORTSCI12202-17

Stansell, Z., Hyma, K., Fresnedo-Ramírez, J., Sun, Q., Mitchell, S., Björkman, T., et al. (2018). Genotyping-by-sequencing of *Brassica oleracea* vegetables reveals unique phylogenetic patterns, population structure and domestication footprints. *Hortic. Res.* 5, 38. doi: 10.1038/s41438-018-0040-3

Sun, X., Bucher, J., Ji, Y., van Dijk, A. D. J., Immink, R. G. H., and Bonnema, G. (2018). Effect of ambient temperature fluctuation on the timing of the transition to the generative stage in cauliflower. *Environ. Exp. Bot.* 155, 742–750. doi: 10.1016/j.envexpbot.2018.06.013

Swarts, K., Li, H., Navarro, J. A. R., An, D., Romay, M. C., Hearne, S., et al. (2014). Novel methods to optimize genotypic imputation for low-coverage, next-generation sequence data in crop plants. *Plant Genome* 7, 0. doi: 10.3835/plantgenome2014.05.0023

Tortosa, M., Cartea, M. E., Rodríguez, V. M., and Velasco, P. (2018). Unraveling the metabolic response of *Brassica oleracea* exposed to *Xanthomonas campestris* pv. *Campestris*. *J. Sci. Food Agric.* 98, 3675–3683. doi: 10.1002/jsfa.8876

Tyagi, S., Sri, T., Singh, A., Mayee, P., Shivaraj, S., Sharma, P., et al. (2019). Suppressor of overexpression of constans1 influences flowering time, lateral branching, oil quality, and seed yield in *Brassica juncea* cv. *Varuna*. *Funct. Integr. Genomics* 19, 43–60. doi: 10.1007/s10142-018-0626-8

Uptmoor, R., Schrag, T., Stützel, H., and Esch, E. (2008). Crop model based QTL analysis across environments and QTL based estimation of time to floral induction and flowering in *Brassica oleracea*. *Mol. Breed.* 21, 205–216. doi: 10.1007/s11032-007-9121-y

Varaud, E., Brioudes, F., Szécsi, J., Leroux, J., Brown, S., Perrot-Rechenmann, C., et al. (2011). AUXIN RESPONSE FACTOR8 regulates *Arabidopsis* petal growth by interacting with the bHLH transcription factor BIGPETALp. *Plant Cell* 23, 973–983. doi: 10.1105/tpc.110.081653

Walley, P. G., Carder, J., Skipper, E., Mathas, E., Lynn, J., Pink, D., et al. (2012). A new broccoli × broccoli immortal mapping population and framework genetic map: tools for breeders and complex trait analysis. *TAG. Theor. Appl. Genet.* 124, 467–484. doi: 10.1007/s00122-011-1721-6

Wang, B., Zhou, X., Xu, F., and Gao, J. (2010). Ectopic expression of a Chinese cabbage brargos gene in *Arabidopsis* increases organ size. *Transgenic Res.* 19, 461–472. doi: 10.1007/s11248-009-9324-6

Xu, X., Luo, W., Guo, J., Chen, H., Akram, W., Xie, D., et al. (2019). Fine mapping and candidate gene analysis of the yellow petal gene *ckpc* in Chinese kale (*Brassica oleracea* L. var. *Alboglabra* bailey) by whole-genome resequencing. *Mol. Breed.* 39, 96. doi: 10.1007/s11032-019-1011-6

Yousef, E. A. A., Müller, T., Börner, A., and Schmid, K. J. (2018). Comparative analysis of genetic diversity and differentiation of cauliflower (*Brassica oleracea* var. *Botrytis*) accessions from two ex situ genebanks. *PLoS One* 13, e0192062. doi: 10.1371/journal.pone.0192062

Zhang, B., Liu, C., Wang, Y., Yao, X., Wang, F., Wu, J., et al. (2015). Disruption of a CAROTENOID CLEAVAGE DIOXYGENASE 4 gene converts flower colour from white to yellow in *Brassica* species. *New Phytol.* 206, 1513–1526. doi: 10.1111/nph.13335

Zhang, F., Wang, H., Kalve, S., Wolabu, T. W., Nakashima, J., Golz, J. F., et al. (2019). Control of leaf blade outgrowth and floral organ development by LEUNIG, ANGUSTIFOLIA 3 and WOX transcriptional regulators. *New Phytol.* 223, 2024–2038. doi: 10.1111/nph.15921

Zhang, Y., Huang, S., Wang, X., Liu, J., Guo, X., Mu, J., et al. (2018). Defective APETALA2 genes lead to sepal modification in *Brassica* crops. *Front. Plant Sci.* 9, 367. doi: 10.3389/fpls.2018.00367

Zheng, M., Hu, M., Yang, H., Tang, M., Zhang, L., Liu, H., et al. (2019). Three BnaIAA7 homologs are involved in auxin/brassinosteroid-mediated plant morphogenesis in rapeseed (*brassica napus* L.). *Plant Cell Rep.* 1–15. doi: 10.1007/s00299-019-02410-4

Zhu, X., Tai, X., Ren, Y., Chen, J., and Bo, T. (2019). Genome-wide analysis of coding and long non-coding RNAs involved in cuticular wax biosynthesis in cabbage (*Brassica oleracea* L. var. *Capitata*). *Int. J. Mol. Sci.* 20, 2820. doi: 10.3390/ijms20112820

**Conflict of Interest Statement:** The authors declare that the research was conducted in the absence of any commercial or financial relationships that could be construed as a potential conflict of interest.